MATHEMATICAL MODELLING OF THERMOCHEMICAL ENERGY STORAGE BY SALT HYDRATES

A thesis submitted in partial fulfilment of the requirements for the award of the degree of

B.TECH

in

Chemical Engineering

By
DHANUSH T (102120026)
KANCHAN GANDIGUDE (102120038)

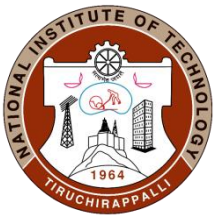

DEPARTMENT OF CHEMICAL ENGINEERING
NATIONAL INSTITUTE OF TECHNOLOGY
TIRUCHIRAPALLI -620015

MAY 2024

MATHEMATICAL MODELLING OF THERMOCHEMICAL ENERGY STORAGE BY SALT HYDRATES

A thesis submitted in partial fulfilment of the requirements for the award of the degree of

B.TECH

in

Chemical Engineering

By

DHANUSH T (102120026)
KANCHAN GANDIGUDE (102120038)

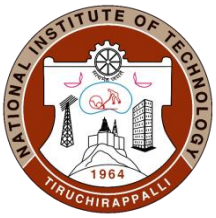

DEPARTMENT OF CHEMICAL ENGINEERING
NATIONAL INSTITUTE OF TECHNOLOGY
TIRUCHIRAPALLI -620015

MAY 2024

BONAFIDE CERTIFICATE

This is to certify that the project titled **MATHEMATICAL MODELLING OF THERMOCHEMICAL ENERGY STORAGE BY SALT HYDRATES** is a bonafide record of the work done by

DHANUSH T (102120026)
KANCHAN GANDIGUDE (102120038)

in partial fulfilment of the requirements for the award of the degree of **BACHELOR OF TECHNOLOGY** in **CHEMICAL ENGINEERING** of the **NATIONAL INSTITUTE OF TECHNOLOGY, TIRUCHIRAPPALLI,** during the year 2023-2024.

DR. JYOTI SAHU
GUIDE

DR.M. ARIVAZHAGAN
HEAD OF DEPARTMENT

Project Viva-voce held on _____

Internal Examiner

External Examiner

TABLE OF CONTENTS

ABSTRACT

This paper explores the efficient storage of thermal energy, crucial for sustainable energy solutions, particularly focusing on the utilization of salt hydrates in thermochemical heat storage systems. Our study involved the development of comprehensive mathematical models to describe the behavior of different salt hydrates under varying conditions. These models were designed to capture the intricate interplay between factors such as temperature, osmotic coefficient, and composition, providing a robust framework for understanding the thermodynamic properties of these materials. Utilizing computational techniques, we solved the formulated mathematical models for a range of salt hydrates. This involved intricate calculations and simulations to simulate the behavior of these materials under different environmental conditions, allowing us to obtain valuable insights into their thermodynamic behavior and phase transitions.

Upon solving the models, we meticulously analyzed the results to determine the percent deviation between our predictions and experimental data for each salt hydrate. Notably, our findings revealed significant variations in deviation among different hydrates, with a particularly interesting trend observed,

The ultimate validation of our study came from comparing our model predictions with experimental data. Encouragingly, our results were found to closely match experimental observations, thereby confirming the accuracy and efficacy of our developed mathematical models. This validation underscores the reliability of our approach and highlights its potential utility in predicting the thermodynamic behavior of salt hydrates with high precision.

Keywords: Thermal energy storage; Salt hydrates; Computational techniques; Phase transitions; Thermochemical heat storage systems.

ACKNOWLEDGEMENTS

Research is considered a learning journey in pursuit of knowledge creation. In this endeavour, it is always fascinating to interact with learned persons, scholars, and academicians to reach the frontier area of subject specialization. On completing this thesis, it is a great pleasure to place on record to acknowledge every soul's valuable and commendable contributions to this research work.

The first and foremost gratitude should go to **DR. G. AGHILA**, Director, National Institute of Technology, Tiruchirappalli, **DR. M. ARIVAZHAGAN** Head of the department, Department of Chemical Engineering and our guide **DR. JYOTI SAHU**, Assistant Professor, Department of Chemical Engineering, National Institute of Technology, Tiruchirappalli, for being our source of inspiration and motivation and for their continuous support throughout our project.

We thank the committee members, **DR. A. ARUNAGIRI, DR. NAGAJYOTI VIRIVINTI** for their valuable guidance and support throughout the project.

We would also like to thank scholars, teaching and non-teaching staff of the department of Chemical Engineering. Our parents, friends who have been constant pillar of support throughout the project work.

LIST OF TABLES

LIST OF FIGURES

ABBREVIATIONS

PCM	Phase change materials
TCM	Thermochemical materials
MP	Modified Pitzer model
PSC	Pitzer–Simonson–Clegg
TGA	Thermogravimetric analysis
TCES	Thermochemical energy storage systems
DSC	Differential Scanning Calorimetry
THT	Thermochemical heat transformers

NOMENCLATURE

MPa	megapascal
GPa	giga pascal
g	grams
kJ	kilo joules
µm	micrometre
mm	millimetre
cm	centimetre
°	degree

CHAPTER 1
INTRODUCTION

Solar energy is more abundant during summer than in winter. The total solar energy supply is sufficient to answer the total demand of energy in dwellings. However, in order to be able to rely completely on sustainable energy sources an efficient method to store energy is required. One of the oldest and simplest way to store thermal energy is in water, for example by using a boiler. For short timeslots this is an efficient and cheap way to store heat [1]. A disadvantage is that a large volume of water is needed and that in spite of insulation, heat will be lost. Thermal storage technologies suitable for building applications are classified in three methods based on the storage principle used: sensible heat (e.g., water tanks, underground storage) [2-4], latent heat (e.g., ice, phase change materials) [5-7] and thermochemical heat storage [8]. The latent heat storage method makes use of a reversible physical or chemical reaction and has higher energy storage density and almost no heat loss, compared to the two other heat storage methods [9]. One promising possibility to store thermal energy is by means of reversible gas solid reactions [10]. Heat is stored into an endothermal dissociation reaction, splitting the thermochemical material into two components (charging), and, at a later time, the energy can be retrieved from the reverse exothermal reaction between the two components (discharging) according to the reaction [11]. An interesting storage material should be low cost, non-toxic, non-corrosive and stable with high energy storage density [12]. These requirements are fulfilled by a number of salt hydrates. In phase change materials (PCMs) heat can be stored by using a phase transition in the material. PCMs have a larger storage capacity than water [13]. A disadvantage is that phase change materials are expensive and still suffer from heat loss during storage, as storage needs to take place at temperature levels that prevent the phase change. In thermochemical materials (TCMs) heat is stored by performing a chemical reaction. TCMs have a large storage capacity and therefore they only require a small volume to store a large amount of heat. As the heat is stored by performing a chemical reaction, there is no loss of heat during storage. The storage volumes required for the annual thermal energy demand of an average household stored in water, PCM and TCM are given by [14]. The most commonly used TCMs are salt hydrates in which thermal energy is stored by drying the salt hydrate and storing the dry salt and the water separately. The reversible reaction of hydration and dehydration of a salt hydrate is shown in Eq. 1.

$$salt.x\,H_2O \overset{heat}{\longleftrightarrow\!\!\rightarrow} salt.yH_2O + (x-y)\,H_2O \qquad (1)$$

The interaction between salt hydrate and water progressively weakens with increasing temperature due to the reduction in the enthalpy of hydrogen bond and finally, above the critical temperature, phase separation occurs [1]. To understand and optimize the phase behaviour, thermodynamic properties of aqueous solutions of Salt hydrates need to be quantified. This requires both the accurate experimental data and a good model which allows prediction of properties of the system in the range of temperature and composition in which experimental data are not available.

Utilizing the Modified Pitzer (MP) model, researchers aim to determine activity coefficients, osmotic coefficients, excess Gibbs energy, and water activity, thereby offering a comprehensive understanding of interactions within ternary systems involving electrolytes, amino acids, and water across a broad concentration and temperature range [15,16]. The interactions discussed primarily entail ion-ion, ion-solute, solute-solute, and solute-solvent interactions, crucial for predicting thermodynamic properties and phase behaviour. This research trajectory extends to investigating the thermodynamic properties of multicomponent aqueous solutions pertinent to environmental contexts. A comprehensive thermodynamic model is proposed to forecast the behaviour of aqueous mixtures containing ions such as Na^+, K^+, Ca^{2+}, Mg^{2+}, Cl^-, and NO^{3-} [17].

Pitzer's seminal work on the ion interaction model, along with its evolved forms like Pitzer–Simonson–Clegg (PSC), serves as the cornerstone for comprehending electrolyte solutions [18,19]. These models offer critical insights into electrolyte behaviour, particularly in techniques like ion-selective electrodes and pH measurements. They meticulously describe the thermodynamic properties of electrolyte solutions, encompassing activity coefficients and osmotic coefficients, pivotal for accurate data interpretation. Moreover, these models furnish a theoretical framework to predict electrolyte behaviours under diverse conditions, thus facilitating the optimization of processes such as chemical reactions, separations, and electrochemical systems. However, their work focuses on symmetrical systems and does not address asymmetrical systems containing ions of different charge types

Khoshkbarchi, Vera, Pazuki, and Sadowski have significantly enriched our comprehension of ternary systems, exemplified by the (NaCl + I^- + proline + water) system, through diverse models and theories [20-22]. Their research elucidates thermodynamic

properties across varying concentrations and temperatures, laying the groundwork for further exploration in this domain. Key properties discussed include activity coefficients, solubility, phase equilibria, and excess properties such as enthalpy and Gibbs energy. These insights play a pivotal role in the design and optimization of processes involving ternary systems, encompassing crystallization, extraction, and separation processes.

Trausel et al. (2014) [14] present compelling evidence that magnesium chloride ($MgCl_2$), sodium sulphide (Na_2S), calcium chloride ($CaCl_2$), and magnesium sulphate ($MgSO_4$) exhibit remarkable potential for thermochemical storage due to their impressive volumetric energy densities. However, further investigation into the properties of salt hydrates is imperative to ensure informed material selection, tailored to diverse operating conditions and requirements. Crucial insights into operational parameters are provided by Clausius-Clapeyron diagrams, while thermogravimetric analysis (TGA) under controlled humidity offers valuable insights into phase diagrams, with equilibrium reached more rapidly under vacuum conditions. Encapsulation using water-permeable polymers may address challenges related to the chemical and physical stability of salt hydrates. Linnow et al. (2014) [23] contribute significantly to understanding hydration kinetics, demonstrating the high theoretical energy densities of $MgSO_4 \cdot 7H_2O$ and $Na_2SO_4 \cdot 10H_2O$. Piperopoulos (2020) [24] further underscores the potential of magnesium sulphate as a storage material, especially for seasonal solar heat storage, given its exothermic hydration reaction. This research collectively propels advancements in thermochemical storage, facilitating efficient and sustainable energy utilization across diverse applications.

In the pursuit of advancing thermochemical energy storage (TCES) systems, multiple research endeavours have emerged to explore various aspects of materials, reactor design, and operational parameters. Gaeini et al. (2019) [25] focus on potassium carbonate as a thermochemical material for heat storage, meticulously investigating its de/re-hydration reactions through kinetic modelling using Thermo-Gravimetric Analysis (TGA) and Differential Scanning Calorimetry (DSC) methods. However, the exclusive concentration on potassium carbonate overlooks the potential of other materials, narrowing the scope of exploration within the field. Furthermore, the study primarily examines the behaviour of potassium carbonate with water vapor, omitting crucial factors like thermal conductivity and system design, which are pivotal for real-world applicability. Similarly, Hawwash et al. (2020) [26] delve into the impact of reactor design on thermal energy storage, particularly focusing on salt hydrates. While their investigation reveals significant insights into how

reactor geometry influences pressure drop, charging time, and thermochemical heat storage, the study's confinement to cylindrical and truncated cone shapes may overlook potential variations in reactor design, urging further exploration into alternative geometries for a comprehensive understanding. Desai et al. (2021) [27] contribute a comprehensive review of TCES systems, emphasizing materials used for sorption and reaction-based TCES, along with discussions on challenges and experimental investigations. However, gaps exist, particularly regarding detailed information on certain TCES materials' safety, stability, and solubility, warranting further exploration and analysis. Conversely, Li et al. (2022) [28] provide numerical insights into the hydration process of a sorbent comprising lithium-based salt hydrate and expanded graphite in a thermal energy storage (TES) module. While offering valuable perspectives on heat and mass migration behaviours, the focus solely on numerical investigation and specific operating conditions may limit the study's ability to fully capture real-world complexities and variations. Hao et al. (2024) [29] propose a multimodule columnar packed-bed reactor for thermochemical heat storage using salt hydrates, showcasing advantages in terms of reaction rate, reaction time, and resistance loss. However, reliance on numerical simulations without experimental validation, coupled with the study's narrow focus on specific reactor design parameters, underscores the need for broader applicability considerations and validation through experimental studies.

Aforementioned salt hydrate models, focus on their application in thermochemical heat transformers (THT) for industrial waste heat recovery, energy storage, and space heating. Studies highlight salt hydrates' high energy storage density, safety, and potential for long-duration storage [30, 31]. Research emphasizes optimizing factors like thermal conductivity, porosity, and system type for efficient heat storage [32]. Kinetic studies explore dehydration/hydration rates, emphasizing the impact of temperature, pressure, particle size, and additives on reaction kinetics [33]. Composite salt hydrates show faster desorption/sorption kinetics, with diffusion being a key limiting factor. The review also discusses the classification of salt hydrate-based systems, reactor design, theoretical models, challenges, and future prospects for salt hydrate-based gas-solid thermochemical energy storage.

A large number of experimental studies have been reported in the literature on the thermodynamic properties of various salt hydrates [34] These include activity of water in the solution, phase separation behaviour and solubility analysis. The data obtained from these studies are well documented by [35]. The most widely used methods for activity

measurements are vapor pressure osmometry [36], laser-light scattering [37], isopiestic method [38], dew point method [39], and sedimentation technique [40],

Regarding the phase separation studies, the coexistence curves for salt hydrates are obtained from the cloud-point data. The cloud point is measured by using either thermos-optical analysis method [41] or through visual observations. Several models have been used for predicting the behaviour of salt hydrates viz. those based on the osmotic virial expansion [42] those based on equations of state [43], and the group contribution schemes [44].

A good thermodynamic model should be able to relate the activity of salt hydrate at low temperatures with its phase behaviour at high temperatures. Unfortunately, models described above use two separate sets of parameters, one to correlate the low-temperature activity data for salt hydrate and the other to correlate the phase separation data. The parameters obtained from the activity data in the low-temperature range (278–343K) are not suitable to predict phase separation and the coexistence curve of salt hydrate systems. This failure stems from inaccuracies in either the model or the experimental data. A very high accuracy of the low-temperature activity data is needed since the data need to be extrapolated over a wide interval of the temperature beyond the range of the measurement and small inaccuracies in the parameter estimates are magnified. Same can be said about the inaccuracies in the model. The task is made difficult by the fact that each activity measurement technique has a relatively narrow range of temperature over which it is accurate. The data obtained using two or more technique needs to be combined in order to extend the range of temperature. This procedure is also a source of error.

Utilizing correlations based on the models, namely the generalized Flory-Huggins theory [45] and the Extended Debye Hückel theory [46], and incorporating activity data obtained from various techniques, an attempt has been made to predict the coexistence curve for the salt hydrate systems in the phase separation region. The work is presented as follows: Firstly, we describe the models governing the thermodynamics of salt hydrate systems. Then, we present the methodology used to estimate the coefficients of these models from the data on the activity of water in the salt hydrate systems. This is followed by the analysis of the results to obtain the model parameters. Finally, the selected model is utilized to grade the quality of the reported solution activity data.

1.1 Objectives of the Study

The main objectives include:

1. Study of phase change of various salt hydrates
2. Study of Charging and Discharging cycles
3. Study of Capacity of batteries
4. Study of thermal management in batteries

CHAPTER 2

LITERATURE REVIEW

M. Gaeini (2018) studied that thermochemical heat storage in salt hydrates is a promising method to improve the solar fraction in the built environment. The major concern at that stage is liquefaction followed by washing out of active material and agglomeration into large chunks of salt, thus deteriorating the diffusive properties of the porous salt hydrate structure. In his work, specific attention is given to the methods to stabilize a sample salt hydrate. Attempts have been made to stabilize calcium chloride by impregnation in expanded natural graphite and vermiculite, and by microencapsulation with ethyl cellulose. The effect of these stabilization methods on the performance of the material, such as kinetics and energy density, has investigated. Characterization of the materials is carried out with combined Thermo-Gravitational Analysis (TGA) and Differential Scanning Calorimetry (DSC) methods and microscopic observation, in order to evaluate the improvements on the basis of three subjects: reaction kinetics, heat storage density and stability

Calcium chloride is found to be one of the promising salt hydrates for thermochemical heat storage for common building applications. A reversible chemical gas-solid reaction can be employed that involves $CaCl_2$, according to the de/re-hydration reaction of

$$CaCl_2 \cdot H_2O(s) + heat \rightleftarrows \ CaCl_2 \cdot (x-y)H_2O(s) + yH_2O\ (g)$$

The interest for calcium chloride has been triggered by: easy availability and subsequently low price, high capacity for water uptake and energy storage density, relatively better chemical stability than other salt hydrates, low corrosiveness and non toxicity. Furthermore, the material dehydrates at low temperature (below 100 °C), which makes it suitable for the applications.

The energy storage density is studied for the four calcium chloride based materials. The energy release for each sample during hydration from anhydrous to hexahydrous state was studied. The simultaneous thermal analysis method allows the estimation of the energy per mole of calcium chloride and per mole of absorbed water. Microencapsulated calcium chloride showed high multicyclic stability, compared with pure and impregnated materials, that liquefy upon hydration under the given conditions. Microencapsulated material remains stable over multiple cycles and shows the fastest kinetics. The only

disadvantage of the encapsulation methodology used in paper is the resulting low energy storage density.

Ard-Jan de Jong (2016) observed that long-term and compact storage of solar energy is crucial for the eventual transition to a 100% renewable energy economy. For that, thermochemical materials provided a promising solution. The compactness of a long-term storage system was determined by the thermochemical reaction, operating conditions, and system implementation with the necessary additional system components. Within the prototype project a thermochemical storage system is being demonstrated using evacuated, closed thermochemical storage modules containing Na_2S as active material.

A significant part of energy to be stored is for space heating and domestic hot water for buildings. Daily storage can be arranged by mature boiler technology, but seasonal storage for at least half a year will require considerably lower heat losses. Besides, seasonal heat storage will usually imply storing very large amounts of heat, so that heat storage should be compact, with high storage density. Energy storage by using solar heat (e.g. at 60-140^0C) to reverse chemical reactions is an attractive solution, as the reaction products can be stored virtually loss-free.

Thermochemical storage offers the potential of loss-free storage with a heat storage density higher than water. The first lab results of the prototype used in this project showed that a storage density of 0.14GJ/m^3 was achieved and they observed that it can expect to reach 0.18GJ/m^3 for coming field tests. In this paper identified and analyzed several possible improvements and show that by mere optimization of the prototype fixed-bed reactor concept using Na_2S, a heat storage density of approximately 1GJ/m^3 can already be achieved.

Michael Graham(2016) studied that thermal energy storage has many important applications, and is most efficiently achieved by latent heat storage using phase change materials (PCMs). Salt hydrates have advantages such as high energy storage density, high latent heat and incombustability. However, they suffer from drawbacks such as incongruent melting and corrosion of metallic container materials. By encapsulating them in a polymer shell, problems can be eliminated. Here we demonstrate a simple method to nanoencapsulate magnesium nitrate hexhydrate, employing an in situ mini emulsion polymerisation with ethyl-2- cyanoacrylate as monomer. Using sonication to prepare mini emulsions improved the synthesis by reducing the amount of surfactant required as

stabiliser. Thermal properties were analysed by differential scanning calorimetry (DSC) and thermogravimetric analysis (TGA). Fourier transform infrared spectroscopy (FTIR) was employed to prove the presence of salt hydrate within the nanocapsules. Results showed the capsules are 100-200nm in size, have salt hydrate located in the core and are stable over at least 100 thermal cycles with only a 3% reduction in latent heat. Supercooling is also drastically reduced

DSC results demonstrated for the first time high thermal stability of the nanoencapsulated salt hydrates, which remained unchanged after 100 thermal cycles with a latent heat of $83.2 Jg^{-1}$. Chemical and macroscale stability of the nanoencapsulated salt hydrates were also proven by FTIR and visual observations after heating/cooling cycles. The thermal properties of the nanocapsules are a great improvement over the bulk $Mg(NO_3)_2 \cdot 6H_2O$, which loses its structural integrity and chemical composition after only 5 cycles.

Salt hydrate PCMs with long lifetimes are important for future energy storage applications, due to their high heat capacity and cost effectiveness compared to commonly used paraffin wax PCMs. Efficient energy storage has the potential to greatly reduce global energy demand, providing a sustainable future

Lin Liang (2017) studied that a new cold storage phase change material eutectic hydrate salt ($K_2HPO_4 \cdot 3H_2O$–$NaH_2PO_4 \cdot 2H_2O$–$Na_2S_2O_3 \cdot 5H_2O$) was prepared, modified, and tested. The modification was performed by adding a nucleating agent and thickener. The physical properties such as viscosity, surface tension, cold storage characteristics, supercooling, and the stability during freeze-thaw cycles were studied. Results showed that the use of nucleating agents, such as sodium tetraborate, sodium fluoride, and nanoparticles, are effective. The solidification temperature and latent heat of these materials which was added with 0, 3, and 5 wt% thickeners were −11.9, −10.6, and −14.8° C and 127.2, 118.6, 82.56 J/g, respectively. Adding a nucleating agent can effectively improve the nucleation rate and nucleation stability. Furthermore, increasing viscosity has a positive impact on the solidification rate, supercooling, and the stability during freeze-thaw cycles.

Luca Scapino (2017) studied that sorption heat storage has the potential to store large amounts of thermal energy from renewables and other distributed energy sources. This article provides an overview on the recent advancements on long-term sorption heat storage at material- and prototype- scales. The focus is on applications requiring heat

within a temperature range of 30–150^{0}C such as space heating, domestic hot water production, and some industrial processes.

Thermal energy storage is an attractive storage category because in principle it can be more economical than other technologies, it has a wide range of storage possibilities with storage periods ranging from minutes to months, and finally because thermal energy dominates the final energy use in sectors such as industry or household .Thermal energy storage can be divided into three main categories according to how energy is stored: sensible heat (e.g. water tanks, underground storage) latent heat (e.g. ice, phase change materials) , and sorption heat storage

Currently, composite materials are investigated because they have the potential to overcome the disadvantages of pure salt hydrates by increasing their hydrothermal stability. This is done by mixing or impregnating salt hydrates with highly porous host matrices or powders. However, problems in heat and mass transport still can arise due to the reduction of empty pores, possible deliquescence and leakage of the salt from the composite, and degradation. To this regard, further research is needed to overcome these problems and to understand extensively the kinetics of a composite material, which does not follow a typical behavior of a salt hydrate nor of an adsorbent. Various prototype reactors and systems were developed by the scientific community to study the performances of sorption materials at macro-scale. Open and closed solid sorption systems have been analyzed and compared. Among the reviewed prototypes, mostly systems based on zeolites were able to achieve temperatures suitable for space heating or DHW production. For these systems, relatively high desorption temperatures were required, unachievable, for example, by conventional solar thermal collectors.

Dongdong Li (2018) studied on the development of a multi-temperature thermodynamically consistent model for salt lake brine systems. Under the comprehensive thermodynamic framework proposed in his previous work, the thermodynamic and phase equilibria properties of the sulfate binary systems (i.e., $Li_2SO_4 + H_2O$, $Na_2SO_4 + H_2O$, $K_2SO_4 + H_2O$, $MgSO_4 + H_2O$ and $CaSO_4 + H_2O$) were simulated using the Pitzer-Simonson Clegg (PSC) model. Various type of thermodynamic properties (i.e., water activity, osmotic coefficient, mean ionic activity coefficient, enthalpy of dilution and solution, relative apparent molar enthalpy, heat capacity of aqueous phase and solid phases) were collected and fitted to the model equations. The thermodynamic properties

of these systems can be well reproduced or predicted using the obtained model parameters.

Farzad Deyhimi (2009) studied the use of Pitzer, PSC as well as an extended PSC ion-interaction approaches for modelling the non-ideal behavior of the ternary HCl + water + 1- propanol systems. These modelling purposes were achieved based on the experimental potentiometric data of a galvanic cell containing a pH glass membrane and Ag/AgCl electrodes. The measurements were performed over the HCl electrolyte molality ranging from 0.01 up to 4.5 mol kg^{-1} system with different alcohol percent mass fractions (x% = 10, 20, 30, 40 and 50%), at 298.15 ± 0.05 K

Pitzer semi-empirical virial coefficient approach has been remarkably successful in modeling the thermodynamic properties of aqueous electrolyte solutions. Although this approach proved to be also a valuable method for correlation and prediction of thermodynamic properties of electrolytes in mixed solvent media, there is still only a limited number of reported studies concerning its application for modeling such systems. Pitzer and Simonson (PS) developed a newer model as well that is applicable over the entire concentration range for the investigation of mixtures containing ions of symmetrical charge type.

Both experimental potentiometric data along with the related model parameters associated with Pitzer, PSC, and an extended PSC approaches concerning the investigation of the ternary HCl + 1- PrOH + water electrolyte system, are for the first time reported in his work.

Edilson C. Tavares (1999) studied the solid-liquid equilibrium in aqueous multi-electrolyte systems using the quasiisothermic thermometric technique (QTT). The principle of the QTT is based on thermal effects associated with the phase transformations that occur in the system. In order to test the apparatus, salt solubility data at 298.15 K for the aqueous systems H_2O+NaCl+KCl, H_2O+NaCl+Na_2SO_4, H_2O+$NiCl_2$+$NiSO_4$ are presented. The data obtained for the three systems are in good agreement with the literature, including solid phase boundaries due to hydration. This agreement indicates the accuracy of the proposed method.

The QTT has been properly tested for the measurement of salt solubilities and solid phase transitions. The apparatus is simple construction and can be operated with the aid of the computer interface, giving accurate data. The burette should be monitored via interface and computer. The QTT has been applied for the measurement of new salt solubility and solid phase transition data for the system $NiCl_2$+$NiSO_4$+H_2O at 298.15 K.

Huinan Wang (2020) Vapor–liquid equilibrium (VLE) data and modeling for LiBr + H_2O and LiBr + $CaCl_2$ + H_2O are reported in this paper. This work focuses on the experimental determination of the boiling point of LiBr + H_2O and LiBr + $CaCl_2$ + H2O solutions with vapor pressures between 6 and 101.3 kPa and the total molality of salt ranging from 0 to 21.05 $molkg^{-1}$. The procedures were carried out in a computer-controlled glass apparatus. The relationship between the boiling point and saturated vapor pressure is obtained, and Xu's model is used to correlate and predict the VLE. By correlation of the data (literature and experimental) for LiBr + H_2O and LiBr + $CaCl_2$ + H_2O, the parameters are obtained. e compared the results with the ElecNRTL model and Pitzer model. The parameters for the LiBr + H_2O, $CaCl_2$ + H_2O, and LiBr + $CaCl_2$ + H_2O systems can be successfully used to calculate and predict the VLE data

Christoph Rathgeber (2019) In this work, the modified BET equations are extended in order to calculate solubility phase diagrams of concentrated salt solutions with relatively high water activities within the range of undersaturation. Predicting solubility phase diagrams of mixtures of salts and water is of interest in various application fields, e.g. in the process of extracting salts or salt hydrates from natural salt brines to develop working fluids in absorption refrigeration systems, or to develop phase change materials for thermal energy storage . As an example, BET parameters of NaCl are determined and applied to calculate solubility phase diagrams of NaCl + H_2O, NaCl + LiCl + H_2O, and NaCl + $CaCl_2$ + H_2O within the temperature range of around 250–500 K. In the ternary systems, the best agreement with solubility data from literature is obtained using constant BET parameters of NaCl and an additional temperature-dependent regular solution parameter to account for salt-salt interaction.

2.2 Various Models Available

Various Thermodynamic models are studied from literature.

a) Debye–Hückel equation

The Debye Hückel equation is a mathematical expression developed to explain certain properties of electrolyte solutions, or substances found in solutions in the form of charged particles (ions). The Debye Hückel equation accounts for the interactions between the different ions, which are the primary cause of differences between the properties of dilute electrolyte solutions and those of so-called ideal solutions.

The Debye-Hückel theory is based on three assumptions of how ions act in solution:

1. Electrolytes completely dissociate into ions in solution
2. Solutions of Electrolytes are very dilute, on the order of 0.01 M
3. Each ion is surrounded by ions of the opposite charge, on average

b) Davies equation

Davies equation is useful at ionic strengths up to 0.5M, making it a better choice than the Deybe-Huckel Model, It makes better calculation in concentrated solutions than Deybe-Huckel Model. This equation was originally published in 1938.The calculation gets deviated from experiment for electrolytes that disassociate into ions with higher charges

c) Pitzer

Pitzer equations were first introduced by physical chemist Kenneth Pitzer. The parameters of Pitzer equations are linear combination of a parameters which differentiate amongst ions and solvent. The parameters are derived from various experimental data such as activity data and salt solubility. The equations are made of an extended Deybe-Huckel limiting law and a virial expansion. Pitzer equations are based on an ion interaction approach, where strong interactions are treated as ion pair formation but weaker interactions are treated as ion-ion interactions that contribute to the respective ions activity coefficients .The Pitzer equations are based on an extension of the Debye-Hückel equation using a virial equation approach, where the interactions between pairs and triplets of ions and molecules are described by empirical parameters. A Pitzer model is therefore dependent on a wealth of experimental data that underlie the database of Pitzer

parameters. Pitzer modelling of the major components of seawater (seawater electrolyte) is well established, and is being applied to trace metals as the relevant experimental data become available.

d) B-E-T Method

BET method is also used for predicting phase change across a range of temperature and concentration. The main parameter used in BET modelling is r and ε. These parameters are temperature dependent. The number of binding sites on salt is represented by r and ε represents the difference between the molar enthalpy of adsorption of water on the salt and the molar enthalpy of liquefaction of water.

e) Pitzer Simonson Clegg

It is one of the most popular models for predicting behavior of mixed electrolytes. In the PSC model, the excess Gibbs energy is represented by summation of short-range and long-range interactions. The long-range forces contribution is represented by the extended DH expression and short-range interaction term is represented by Margules expansion which includes the parameters for the interaction of solvent -anion, solvent-cation, and the disassociation of all electrolytes.

2.3 Research gap

There is wide research gap in the Salt hydrates such as

1. Lack of experimental data at high temperature and pressure and validation,
2. Model accounting for salt hydrates at elevated temperature, pressure, and concentration
3. Accounting of unstable chemical reactions
4. Accounting of complex phase equilibria (vapor: liquid: solid).

CHAPTER 3

METHODOLOGY

3.1 Model

The osmotic coefficient (φ) of an aqueous electrolyte is related to the chemical potential of water, (μ_w), as follow:

$$\varphi = -\frac{\mu_w - \mu_w^0}{M_W RT \upsilon m} \quad (1)$$

where, μ^0_w is the chemical potential of water in its standard state. M_w is the molecular mass of water. υ is the number of ions produced on dissociation of one molecule of the electrolyte. m is the molality of the electrolyte solution, R is the gas constant, and T is the absolute temperature. These variables collectively determine the extent of deviation from ideal behaviour in solutions, providing insights into the behaviour of solutes and solvents in solution dynamics.

In this work, total Gibbs free energy of the system is given by summation of long range (Lr) and short-range interactions (Sr), i.e.,

$$\frac{F}{RT} = \frac{F^{Lr}}{RT} + \frac{F^{Sr}}{RT} \quad (2)$$

Long range interaction, is also termed as electrostatic interaction is given by Pitzer`s form of the Debye- Huckle (PDH) function,

$$\frac{F^{Lr}}{RT} = -(v_w n_w + \upsilon v_s n_s)\frac{4A_\varphi I_x}{b} ln \ln\left(1 + bI_x^{\frac{1}{2}}\right) \quad (3)$$

where, n_w, n_s are the number of moles of water, salt respectively. v_s, v_w are the partial molar volume (m^3/mole) of salt, solvent respectively. b is the closest approach parameter. Total no. of ions per salt is defined by $\upsilon = \upsilon_M + \upsilon_X$. I_x is the ionic strength.

In eqn. 3, Debye Hückel type constant A_φ is defined as function of the dielectric constant of water as follows,

$$A_\varphi = \frac{1}{3}\left[\frac{2\pi N_A}{V_S}\right]^{\frac{1}{2}}\left[\frac{e^2}{4\pi\varepsilon D_S KT}\right]^{\frac{3}{2}} \quad (4)$$

where M_w is molecular weight of solvent i.e., water in gram/mol, N_A is Avogadro number, K is Boltzmann constant, ε is permittivity of vacuum, e is electronic charge, D_S is dielectric constant of water, V_S is the molar volume of water.

In eqn. 3, the ionic strength, I_x is defined as function of the molarity as follows,

$$I_x = \sum C_i \frac{Z_i^2}{2} \text{ or } I_x = \frac{1}{2} Cv|Z_+ Z_-| \quad (5)$$

The expression for the short-range interaction contribution of aqueous salt solution is obtained from Generalized Flory- Huggins theory as given below,

$$\frac{F^{Sr}}{RT} = v_w n_W \, ln \ln \phi_w + v v_s n_s \, ln \ln \phi_s + \chi_{sw} v_w n_w \phi_s \quad (6)$$

In eqn. (6), volume fraction of the salt hydrate ϕ_S is define as

$$\phi_S = \frac{v v_s n_s}{v_w n_W + v v_s n_s} \quad (7)$$

In eqn. (6), The term χ_{sw} is the generalized Flory-Huggins parameter and should be regarded as a function of the volume fraction of the salt hydrate ϕ_S, and temperature, T of the system. By combining Eqn. 2, 3, & 6, total Gibbs free energy of the system is given as,

$$\frac{F}{RT} = -(n_w + \nu n_s) \frac{4A_x I_x}{b} ln\left(1 + bI_x^{\frac{1}{2}}\right) + n_w ln\phi_w + \nu n_s ln\phi_s + \chi_{sw} \, n_w \phi_s \quad (8)$$

where, n_S and n_w represent the moles of salt hydrate and water in salt hydrate solution, respectively.

Derivative of Equation (8) w. r. t. moles of water and salt gives us chemical potential of water and salt hydrate respectively.

$$\frac{\mu_w - \mu_w^0}{RT} = \left(\frac{\delta \frac{F}{RT}}{\delta n_w}\right)_{n_s} = \left(I_x ln\left(1 + bI_x^{\frac{1}{2}}\right)\right)\left[-\frac{\nu n_s}{n_w}\right] - \frac{(n_w + \nu n_s)}{2\left(1 + bI_x^{\frac{1}{2}}\right)} \frac{I_x^{-\frac{1}{2}}}{n_w} + ln\phi_w +$$

$$\phi_s \left(1 - \frac{v_w}{v_s}\right) - \chi_{sw} \phi_s^2 - \frac{\delta \chi_{sw}}{\delta \phi_s} \phi_s^2 (1 - \phi_s) \quad (9)$$

$$\frac{\mu_s-\mu_s^0}{RT}=\left(\frac{\delta\frac{F}{RT}}{\delta n_s}\right)_{n_s}=I_x ln\left(1+bI_x^{\frac{1}{2}}\right)\left(2+\frac{n_w}{n_s}\right)+\left(\frac{n_w}{n_s}+\nu\right)\left(\frac{1}{\left(1+bI_x^{\frac{1}{2}}\right)}\ b\frac{1}{2}I_x^{\frac{3}{2}}\right)+$$

$$v\ [ln\ \ln\phi_s+\left(1-\frac{v_S}{v_w}\right)\ \phi_w+\frac{v_s}{v_w}\ \chi_{sw}(1-\phi_s)^2+\frac{v_s}{v_w}\phi_s(1-\phi_s)^2\ \frac{\delta\chi_{sw}}{\delta\phi_s}\qquad(10)$$

The criteria governing phase equilibrium between two distinct phases (referred to as the α phase and β phase) are specified by

$$\mu_w^\alpha=\mu_w^\beta\qquad(11)$$

$$\mu_S^\alpha=\mu_S^\beta\qquad(12)$$

By substituting Equations (9) and (10) into Equations (11) and (12), we derive the following equations that govern the phase equilibria.

$$\frac{ln(1-\phi_s^\alpha)}{ln(1-\phi_s^\beta)}+\left(\ \phi_s^\alpha-\phi_s^\beta\right)\left(1-\frac{v_w}{v_s}\right)-\left[\chi_{sw}(T,\phi_s^\alpha)\ \phi_s^{2\alpha}+\frac{\delta\chi_{sw}(T,\phi_s^\alpha)}{\delta\phi_s^\beta}\phi_s^{2\alpha}(1-\phi_s^\alpha\ )\ \right]-$$

$$\left[\chi_{sw}\left(T,\phi_s^\beta\right)\phi_s^{2\beta}+\frac{\delta\chi_{sw}\left(T,\phi_s^\beta\right)}{\delta\phi_s^\beta}\phi_s^{2\beta}\left(1-\phi_s^\beta\ \right)\right]=0\qquad(13)$$

$$v\ \left[+\left(1-\frac{v_S}{v_w}\right)\ \left(2-\phi_s^\alpha-\phi_s^\beta\right)\ \right]+$$

$$\left[\frac{v_s}{v_w}\ \chi_{sw}\ (T,\phi_s^\alpha)(1-\phi_s^\alpha)^2+\frac{v_s}{v_w}\phi_s^\alpha(1-\phi_s^\alpha)^2\ \frac{\delta\chi_{sw}(T,\phi_s^\alpha)}{\delta\phi_s^\alpha}\right]+\left[\frac{v_s}{v_w}\ \chi_{sw}\left(T,\phi_s^\beta\right)\left(1-\phi_s^\beta\right)^2+\right.$$

$$\left.\frac{v_s}{v_w}\phi_s^\beta\left(1-\phi_s^\beta\right)^2\ \frac{\delta\chi_{sw}\left(T,\phi_s^\beta\right)}{\delta\phi_s^\beta}\right]=0\qquad(14)$$

The values of ϕ_s^α and ϕ_s^β at a specific temperature *T* are obtained by solving Equations (13) and (14) simultaneously. The critical point is determined by the following condition:

$$\frac{\delta^2(\mathrm{F}/RT)}{\delta\phi_s^2}=\frac{\delta^3(\mathrm{F}/RT)}{\delta\phi_s^3}=0\qquad(15)$$

The critical temperature, T_c , and critical salt hydrate volume fraction, ϕ_{sc}, are determined by solving the above two equations simultaneously.

3.2 Procedure for regression of the model parameters

The parameter χ_{sw} in the Flory-Huggins theory governs the interaction between salt and water, thus determining the thermodynamic characteristics of Salt hydrate systems. Various correlation forms for this parameter have been documented in the literature [47-50]. In this analysis, we explore the empirical form of χ_{sw} as follows:

$$\chi_{sw}(T, \phi_S) = \sum_{i=0}^{n} b_i(T)\phi_S^i \quad (18)$$

$b_i(T)$ is temperature dependent coefficient and as expressed as:

$$b_i(T) = b_{i\alpha} + b_{i\beta}\left(\frac{1}{T} - \frac{1}{T_r}\right) + b_{i\gamma}\, ln\left(\frac{T}{T_r}\right) \quad (19)$$

where, $b_{i\alpha}, b_{i\beta}$ and $b_{i\gamma}$ are constants.

This form necessitates determining 3(n+1) empirical constants using the experimental data. For this representation of $\chi_{sw}(T, \phi_S)$, we have

$$\frac{\partial \chi_{sw}(T,\phi_S)}{\partial T} = \sum_{i=0}^{n} \frac{\partial b_i}{\partial T}\phi_s^i = \sum_{i=0}^{n}\left(-\frac{b_{i\beta}}{T^2} + \frac{b_{i\gamma}}{T}\right)\phi_s^i \quad (20)$$

And

$$\frac{\partial^2 \chi_{sw}(T,\phi_S)}{\partial \phi_S \partial T} = \sum_{i=0}^{n} i\,\frac{\partial b_i}{\partial T}\phi_s^{i-1} = \sum_{i=0}^{n} i\left(-\frac{b_{i\beta}}{T^2} + \frac{b_{i\gamma}}{T}\right)\phi_s^{i-1} \quad (21)$$

We observe from the above equations that coefficients $b_{i\alpha}$ are eliminated during the partial differentiation of χ_{sw} with respect to temperature. To estimate the constants, we solely rely on the data concerning the osmotic coefficient of water in salt hydrate systems across a range of temperatures and compositions for the regression of all the constants.

Three different values of n, namely n = 3 and 4 are utilized to assess the impact of n (the degree of polynomial in ϕ_s in Equation (18)) on the quality of the estimates. The nonlinear least-square method of Levenberg-Marquardt is employed for regression in all cases. The l^2-norm of the residual (||R||) is employed to evaluate the quality of the regression. It is defined as:

$$\|R\| = \left[\sum_{j=1}^{ndata}\left(\frac{r_j^{exp} - r_j^{model}}{\sigma_j}\right)^2\right]^{1/2} \quad (22)$$

where r_j^{exp} and r_j^{model} (j = 1,….., n data) respectively denote the experimental value and the corresponding model prediction of the quantity to be fitted (osmotic coefficient data), and σ_j is the standard deviation.

CHAPTER 4

RESULTS AND DISCUSSION

We initially examine the outcomes of the regression analysis conducted on the data utilizing the proposed method. This methodology relies solely on the osmotic coefficient data. Within the existing literature, there are limited studies that quantify the activity of water (osmotic coefficient) in salt hydrates across a broad spectrum of temperatures and concentrations. The activity of water, determined through sedimentation technique [10], is accessible within the temperature span of 293–313 K, while that derived from vapor pressure osmometry [6] is attainable within the range of 308–338 K.

The table-1 list the l^2-norm of the residuals, ||R||, for the best fit values of the constants. It is seen that the value of ||R|| for n = 1 is significantly larger than those for n = 2 , 3 and 4. Hence the linear form (n = 1) is not used in the further analysis. The values of ||R|| for n = 3 and 4 are not significantly different from each other and hence both are accepted.

Table-4.1 - l^2-norm of the residuals, ||R||, for the best fit values of the constants for our work to the experimental data

Salt Hydrates	n = 1	n = 2	n = 3	n = 4
NaCl	38.2962	1.70324	1.402143	1.00947
LiCl	67.1905	10.85738	6.976521	1.479885
$CaCl_2$	49.3203	6.616037	1.918884	0.615101
Li_2SO_4	81.5631	6.766015	3.255115	1.160013
$MgSO_4$	84.14794	9.856403	4.550855	2.99597

Table 2 lists the regression estimates of the constants $b_{i\alpha}$, $b_{i\beta}$ *and* $b_{i\gamma}$ **,** (i=0, 1, . . ., n), for n = 3. Table 3 lists the regression estimates of the constants $b_{i\alpha}$, $b_{i\beta}$, $b_{i\gamma}$ *and* $b_{i\delta}$ (i=0, 1, . . ., n), for n = 4.

Table-4.2 The least square estimates of constants $b_{i\alpha}$, $b_{i\beta}$ and $b_{i\gamma}$, obtained from osmotic coefficient data for n = 3

	NaCl	**LiCl**	**Li_2SO_4**	**$MgSO_4$**	**$CaCl_2$**
a	79.25810001	-13416.83325	1805.607702	41812.72232	6917.205725
b	0.392577746	-13655.82569	-1.52985731	-1710403.759	-2045.137046
c	406.7499327	1438.11892	-162.818885	-124710.7606	-40191.75976
d	79.25813745	-17830.20198	1804.459355	25437.18659	8303.19844
e	0.393322704	1813.197152	-1.53831223	-1693135.758	-6.0165132628
f	406.7499327	1840.796406	-314.8768451	114649.0606	38116.51935
g	-461.7558628	216895.324	-16834.84598	-49205.42678	-55686.377
h	-1.299947942	15369.79572	-5.859168109	3900142.407	1578.732542
i	-2712.455354	-25218.75124	-5264.96013	5674.916688	7106.784597
j	-286.6609284	-200587.7443	-73341.05538	-57730.37146	109013.936
k	-0.825744651	-92.36609842	-3.144404132	75602.14676	-3999.432868
l	-1677.795905	6619.358175	4942.140603	4823.346649	-22960.88857

Table-4.3 The least square estimates of constants $b_{i\alpha}$, $b_{i\beta}$, $b_{i\gamma}$ and $b_{i\delta}$ obtained from osmotic coefficient data for n = 4

	NaCl	LiCl	Li_2SO_4	$MgSO_4$	$CaCl_2$
a	-0.212294839	-8475.14118	1583.531513	735.2502247	8261.720861
b	-335.4371663	1.951984408	-1.523361753	-0.791706136	0.574569962
c	10342.4994	11063.71503	335.0484774	-175.5402835	-2205.145069
d	-0.207433846	-8762.679933	1586.790475	735.2499917	8514.638057
e	-323.2401916	1.945589229	-1.521177232	-0791302324	0.57414814
f	-35421.30669	-5249.227446	309.9047436	-175.5427682	637.5750879
g	-4.150170132	139528.488	-21459.34288	6263.204201	-64139.42738
h	357.187306	-2.140533011	-5.649620842	-1.789600289	-1.661789026
i	3024.992372	-42267.20539	-16192.5649	-3417.892075	1822.071307
j	-1.176700102	-28829.39158	-51230.10337	-10121.37875	119035.627
k	9279.052789	-3.087335404	-3.048952414	-1.185368643	-1.257998805
l	0	49056.73421	52595.85194	2229.518494	-1687.598625
m	102073.3323	-139583.3918	-4265.223202	-1750.261638	5734.631344
n	-0.353976317	-2.475147526	-1.159889792	-0.569492703	-0.617783764
o	-33101.67039	-35949.50214	-78519.87037	-6399.459638	-28747.96172

A single temperature (considered the base temperature) serves as the data point. Given that activity data are derived from various measurement techniques, a selection must be made. Three criteria guide the choice of the most suitable data. Firstly, the quality of regression is assessed based on the l^2-norm. Secondly, the accuracy of predicting critical constants, namely Tc and ϕ_{sc} (the critical volume fraction of salt hydrate), utilizing the estimated parameters is evaluated. These critical constants are determined by solving Eqs. (16) and (17) concurrently. Thirdly, the precision of predicting the binodal curve is considered. The binodal curve is approximated by simultaneously solving Eqs. (13) and (14).

We use sets of parameters from Table-4.2 and Table-4.3 to predict the Phase diagram of salt hydrates. In Figure 1, the predicted binodal curves for n = 3, 4 are juxtaposed with experimental data for salt hydrates. Notably, the predicted Phase diagram aligns remarkably well with the experimental observations, particularly when utilizing the parameter set derived from activity data. This congruence underscores the reliability of the predictive model in accurately capturing the phase behaviour of the salt hydrates. The accuracy of the correlation is illustrated through parity plots.

An attempt was made to expand the current correlation to forecast the closed-loop phase diagraph for various Salt hydrates, as illustrated in Figure 6. However, it is evident that the phase diagraph predicted by the model does not enclose the upper critical temperature. One potential explanation for this deviation lies in the failure of our assumption regarding the independence of v_s/v_w (volume of salt/volume of water) concerning temperature, pressure, and salt composition. The assumption of constant v_s/v_w is likely to hold true for temperatures up to and around the lower critical temperature as previous studies have demonstrated its independence from pressure across a broad range [51]. Nonetheless, this assumption may not remain valid beyond this range. Indications suggest that v_s/v_w (volume of salt/volume of water) is independent of pressure, particularly around the lower critical temperature, as evidenced by its stability across a broad pressure range. However, the upper critical temperature aligns closely with the critical point of water (647.1K), which is anticipated to decrease further with the addition of salt hydrate, potentially converging with the upper critical temperature. Given the significant density changes anticipated near the upper critical temperature, it is likely that the v_s/v_w ratio becomes markedly more sensitive to both pressure and temperature in this vicinity. Unfortunately, density data for this system near the upper critical temperature are currently unavailable, preventing verification of this hypothesis.

4. 1) NaCl

A. PARITY PLOT GRAPHS

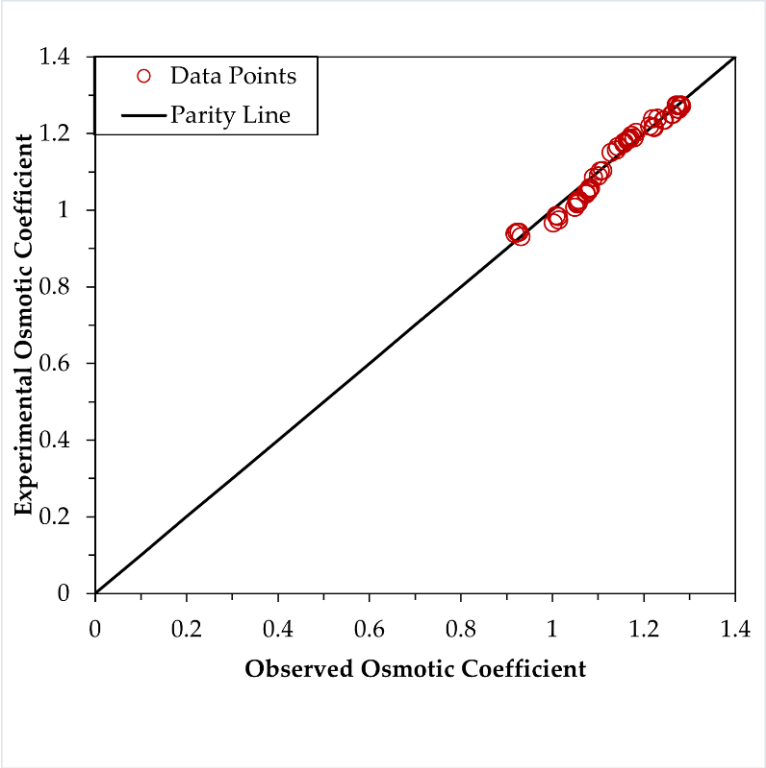

Fig 4.1. Parity plot of NaCl for N=2

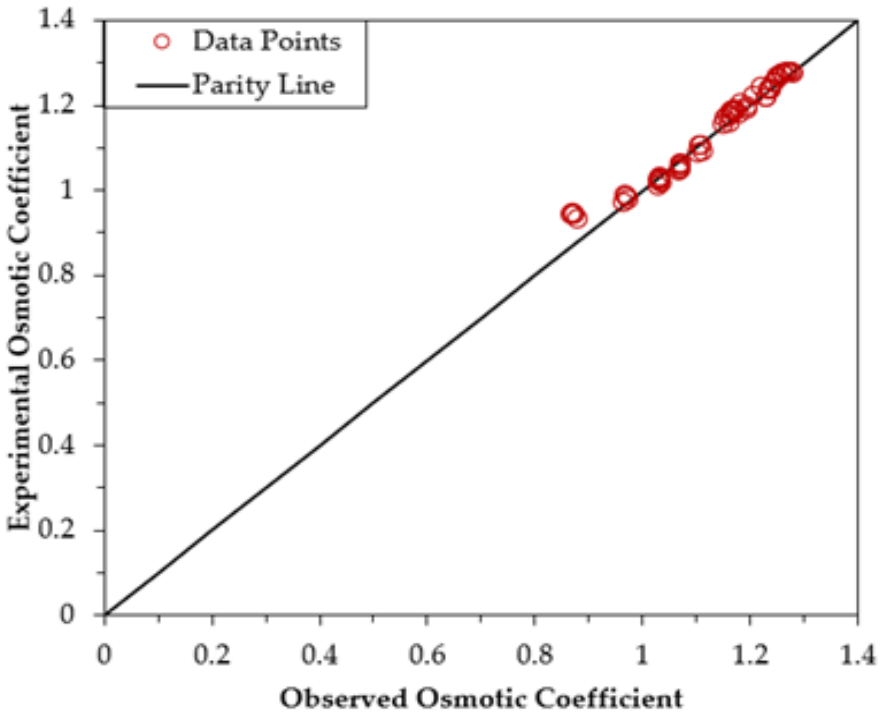

Fig 4.2. Parity plot of NaCl for N=3

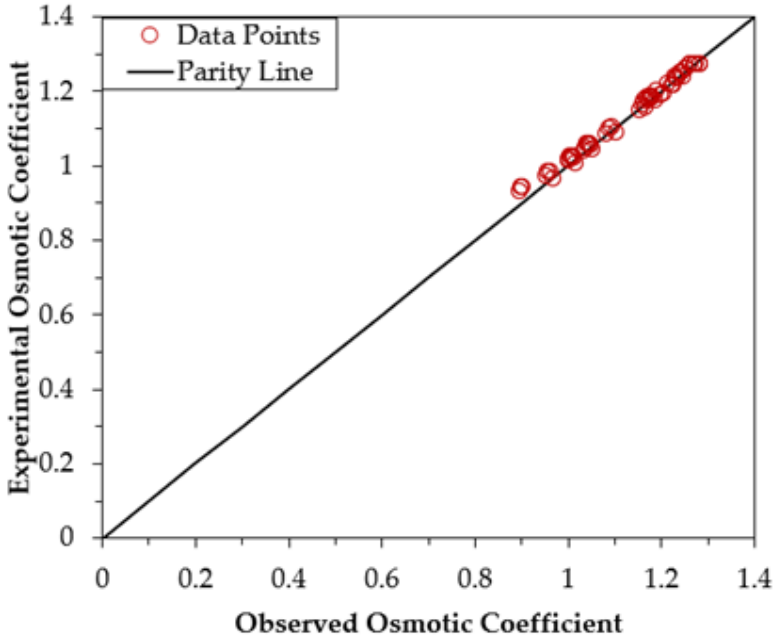

Fig 4.3. Parity plot of NaCl for N=4

B. PHASE DIAGRAM GRAPHS

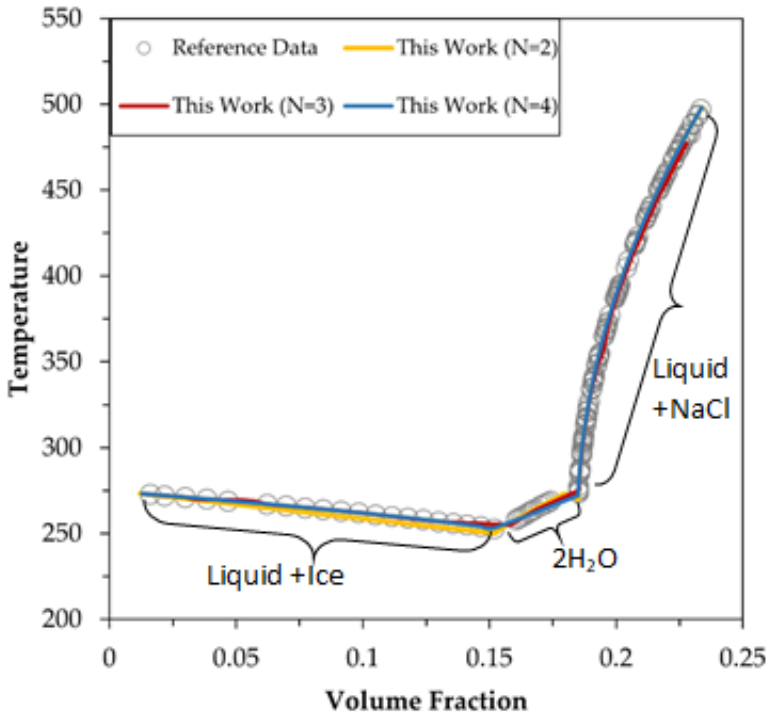

Fig 4.4. Phase diagram of the NaCl + H_2O system
Symbols: experimental data reported in reference data [52-53]. Lines: the present model results.

Fig 4.4. represents the phase diagram of NaCl + H_2O system. The diagram shows areas that represent a particular mixture of salt of NaCl and water at a given temperature. The point at a temperature of 253K is called eutectic point, which is the lowest temperature at which a liquid phase is stable at a given pressure. It's when a solid solute, a solid solvent, and a liquid mixture all exist in the same phase. The eutectic point is also known as the eutectic temperature and is the lowest possible melting point over all of the mixing ratios of the constituents. The temperature range of 253K to 272K represents the $NaCl.2H_2O$ + liquid system which means that you have a rock salt crystal with water molecules as a kind of dissolved impurity ($2H_2O$ molecules occupying the place of one NaCl unit), whereas the temperature this represents the NaCl + liquid system. The complete solid – liquid equilibrium data is traced almost exactly with experimental values for N=2, N=3 and N=4 lines.

4.2) LiCl

A. PARITY PLOT GRAPHS

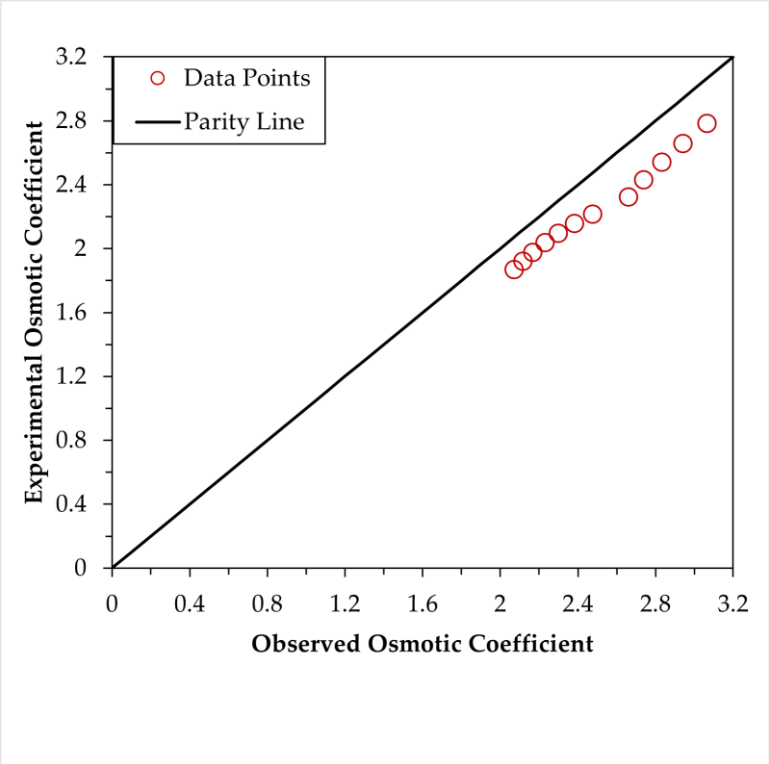

Fig 4.5. Parity plot of LiCl for N=2

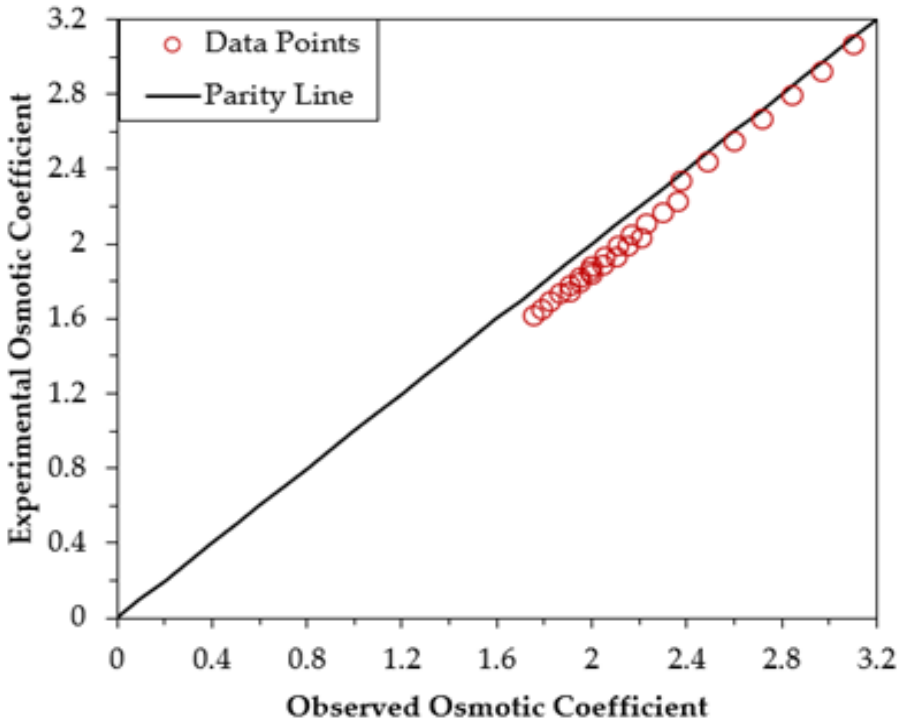

Fig 4.6. Parity plot of LiCl for N=3

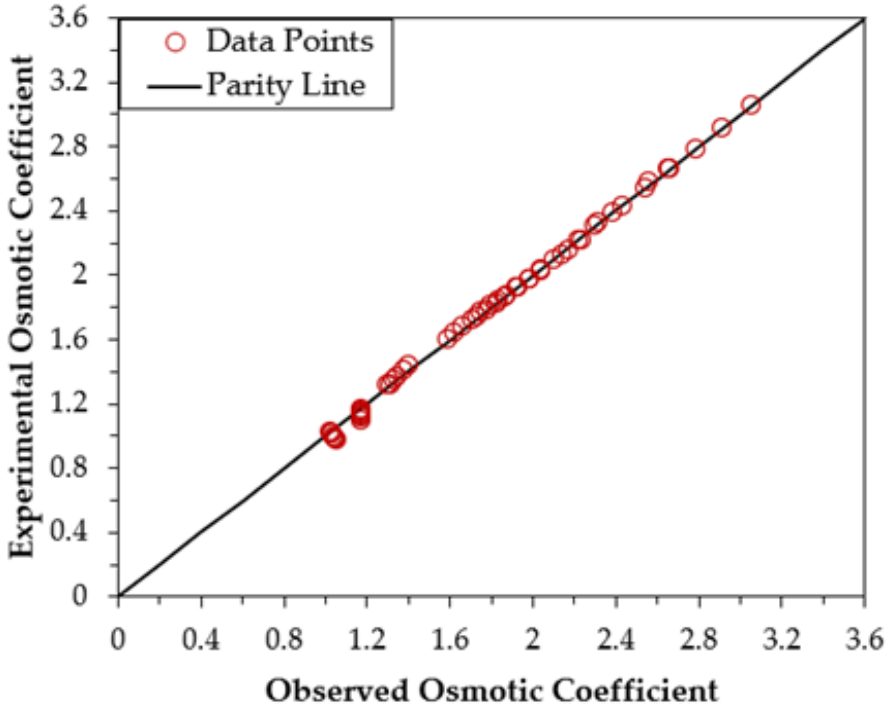

Fig 4.7. Parity plot of LiCl for N=4

B. PHASE DIAGRAM GRAPH

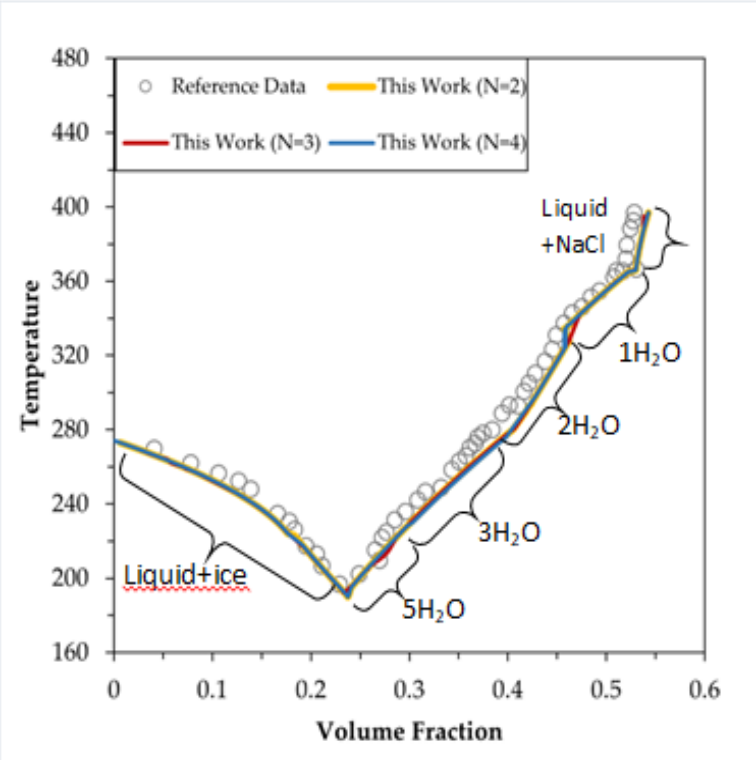

Fig 4.8. Phase diagram of the Li_2SO_4+H_2O system.
Symbols: experimental data reported in reference data [52-54]. Lines: the present model results.

Fig 4.8 represents the phase diagram for LiCl + H_2O system. Besides anhydrous LiCl, there exist four solid lithium chloride hydrates, with respectively 1, 2, 3, and 5 water molecules. These salts are extremely soluble in water. For example, the solubility of the monohydrate LiCl.H_2O is about 20 mol/kg of H_2O in pure water at 273 K. At the eutectic temperature of the LiCl + H_2O system (199 K), which is one of the lowest of all alkali + water or alkaline earth + water systems, the stable solid is the pentahydrate LiCl.5H_2O. Despite this very low temperature, the concentration of the saturated solutions is very high, 24% volume fraction of salt at the eutectic. The calculated liquidus in the LiCl + H_2O system showed good agreement with the experimental results for N=2, N=3 and N=4 lines.

4.3) $CaCl_2$

A. PARITY PLOT GRAPHS

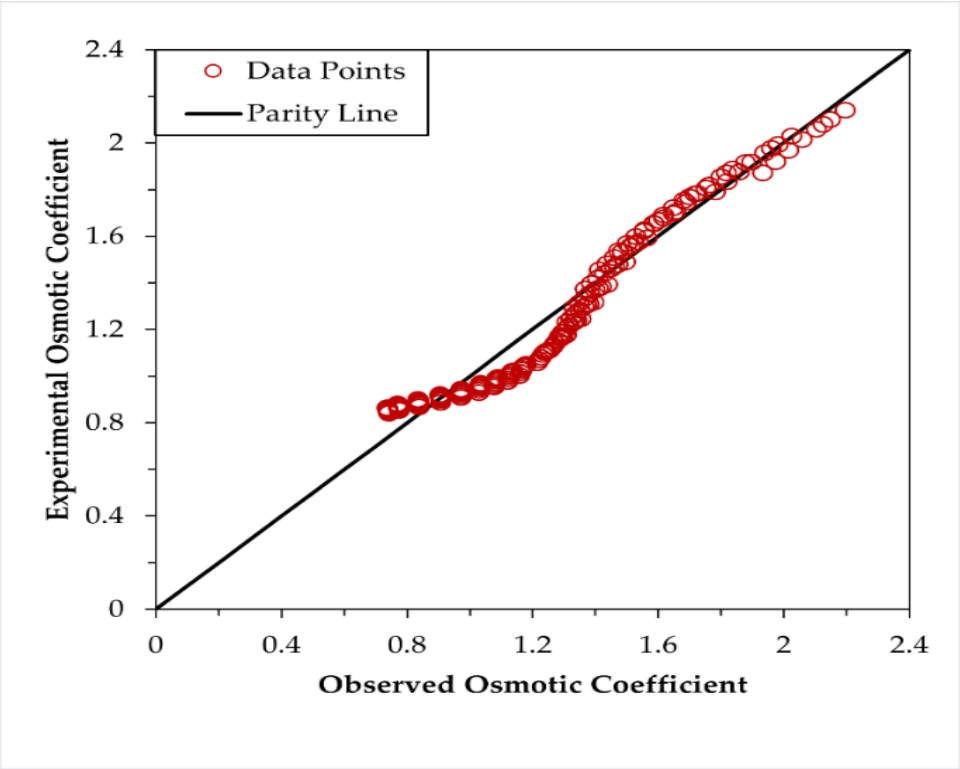

Fig 4.9. Parity plot of $CaCl_2$ for N=2

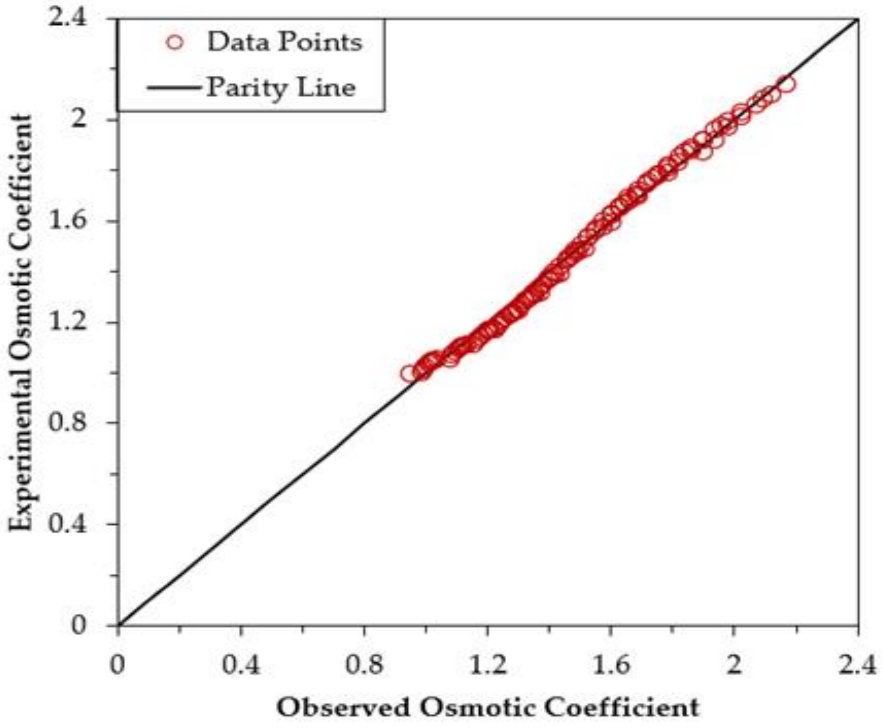

Fig 4.10. Parity plot of $CaCl_2$ for N=3

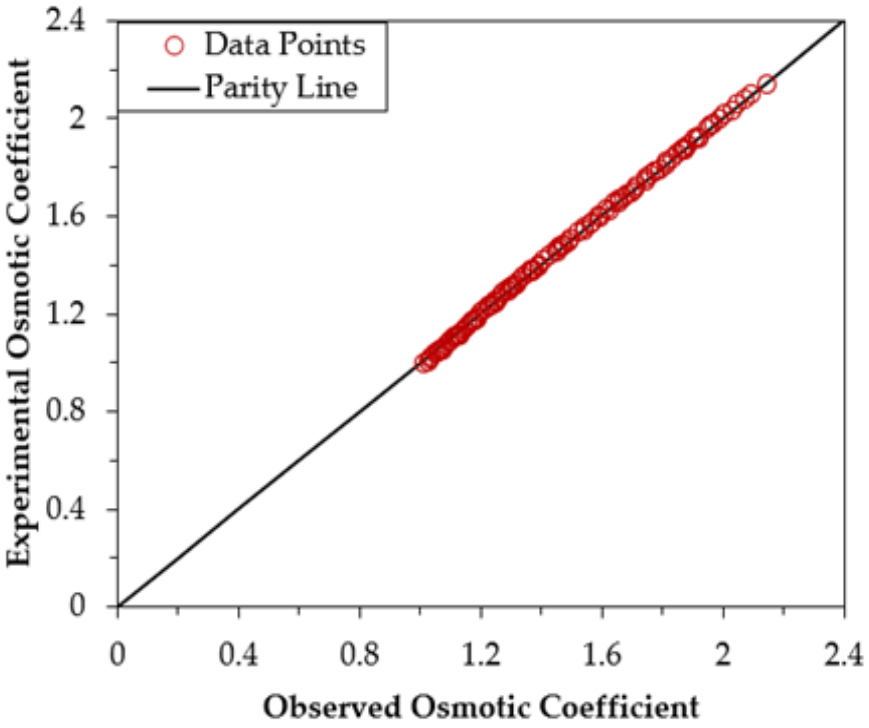

Fig 4.11. Parity plot of $CaCl_2$ for N=4

B. PHASE DIAGRAM GRAPH

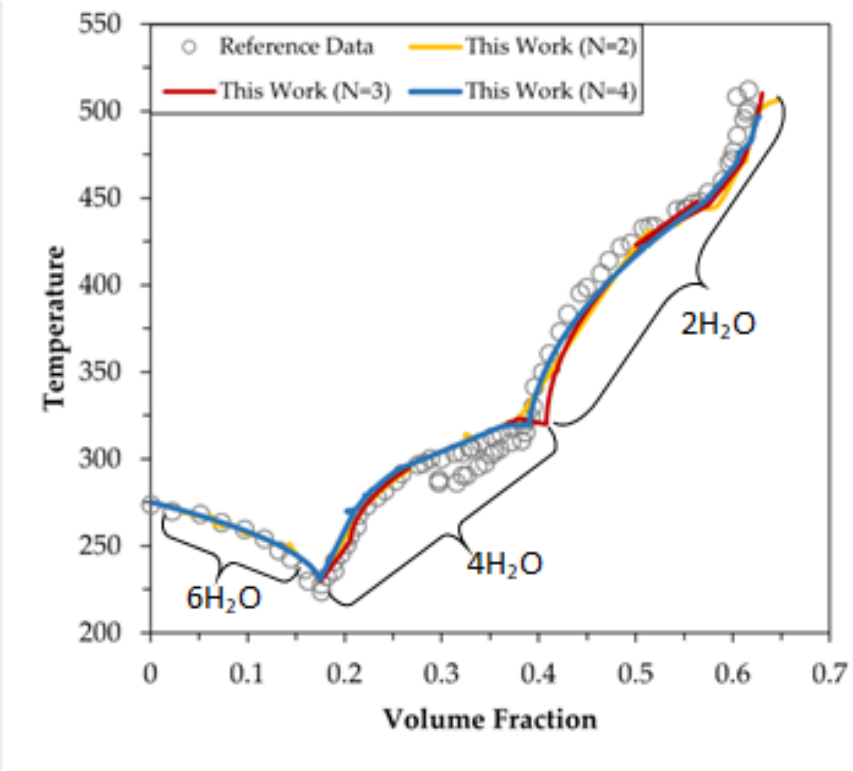

Fig 4.12. Phase diagram of the $CaCl_2 + H_2O$ system
Symbols: experimental data reported in reference data [55-59]. Lines: the present model results.

Fig 4.12. represents the phase diagram for $CaCl_2$ + H_2O system. Phases at equilibrium for the chemical system $CaCl_2$ + H_2O are shown as a function of volume fraction of $CaCl_2$ salt and temperature. There are three solid $CaCl_2$ hydrates of 2, 4 and 6. In which $CaCl_2.6H_2O$ and $CaCl_2.2H_2O$ occur naturally and have mineral names which are called as antarctictites and sinjarites respectively. The eutectic point of this system is around 223.5K. Till the volume fraction of 0.4, our model showed an excellent agreement with the experimental data for N=2, N=3 and N=4 lines,

4.4) Li_2SO_4

A. PARITY PLOT GRAPHS

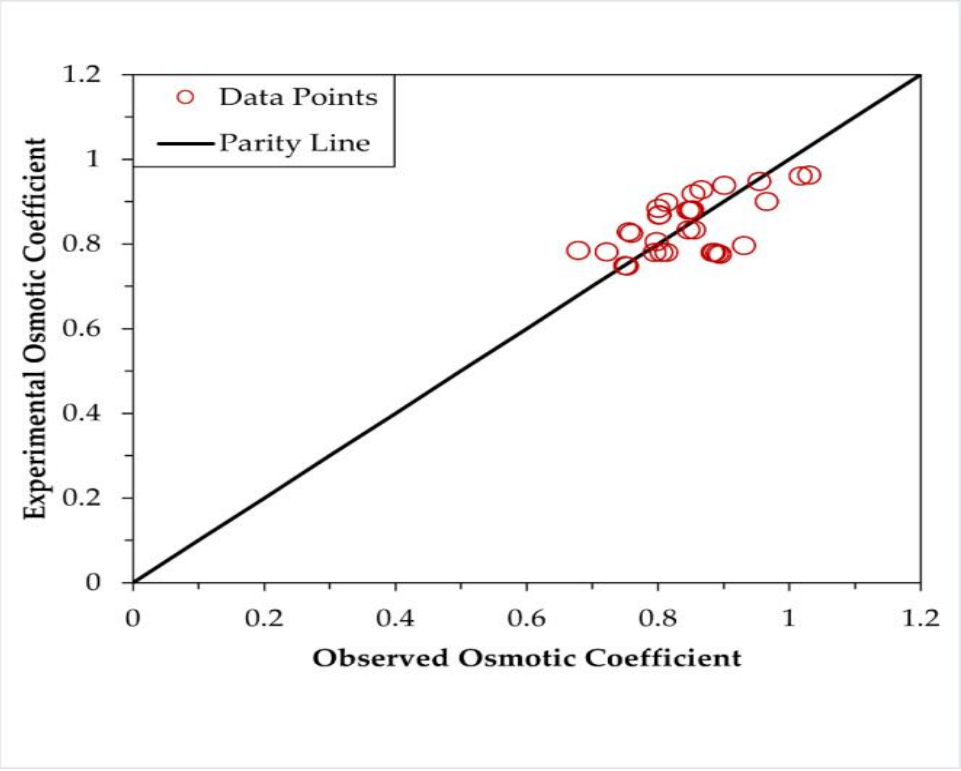

Fig 4.13. Parity plot of Li_2SO_4 for N=2

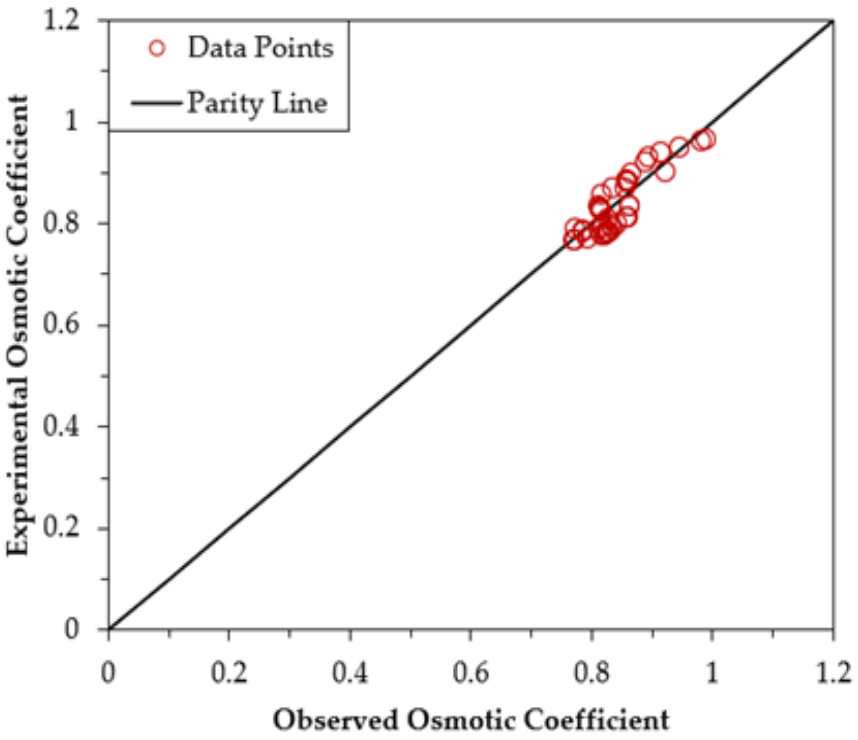

Fig 4.14. Parity plot of Li_2SO_4 for N=3

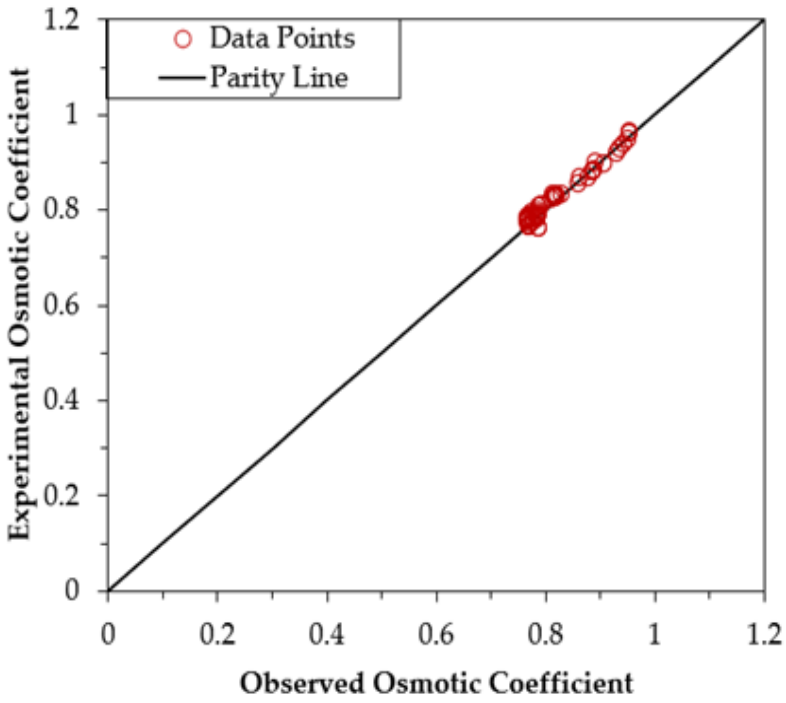

Fig 4.15. Parity plot of Li_2SO_4 for N=4

B.PHASE DIAGRAM GRAPH

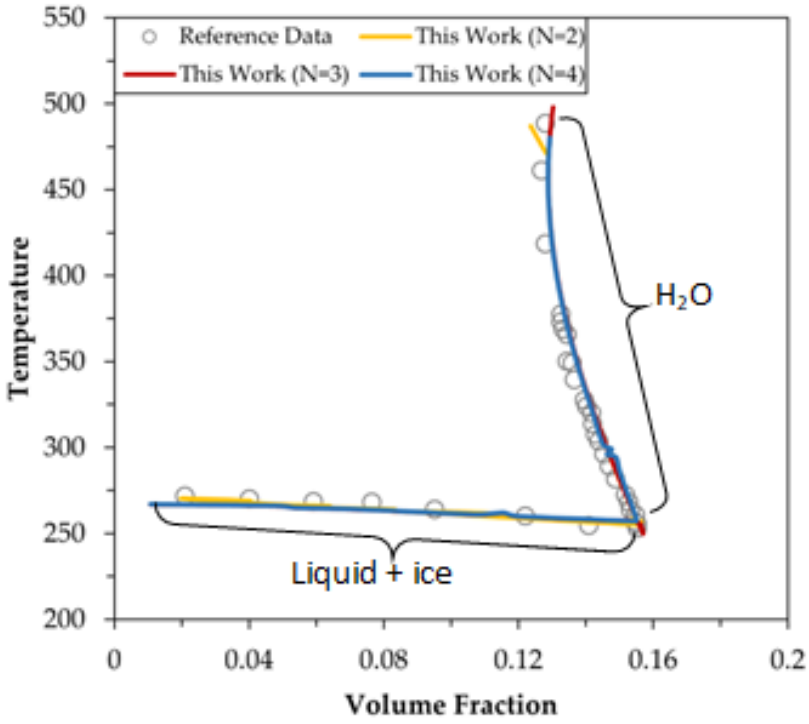

Fig 4.16. Phase diagram of the Li_2SO_4+H_2O system.
Symbols: experimental data reported in reference data [52-54]. Lines: the present model results.

Fig 4.16. represents the phase diagram of Li_2SO_4 + H_2O system. This system depicted a simple curve. There is a slight increase in the solubility of Li_2SO_4 till the eutectic point of around 250K. Here there exist only one form of hydrate salt which is $Li_2SO_4.H_2O$. Our model made an excellent argument in terms of tracing the experimental values with our model values for N=2, N=3 and N=4.

4.5) $MgSO_4$

A. PARITY PLOT GRAPHS

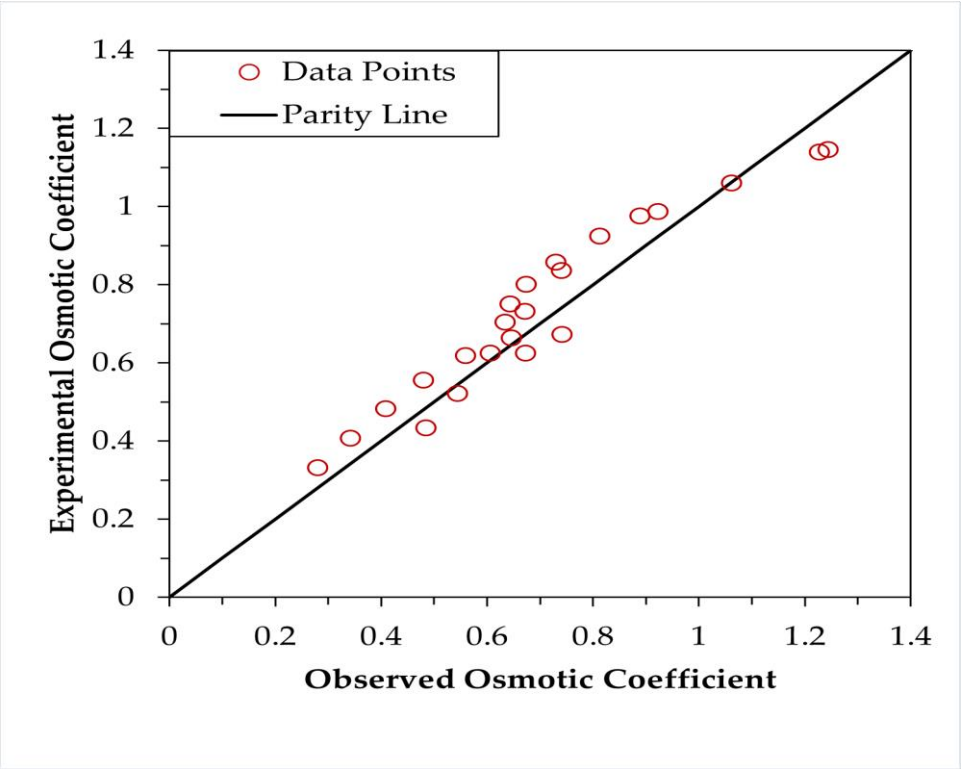

Fig 4.17. Parity plot of $MgSO_4$ for N=2

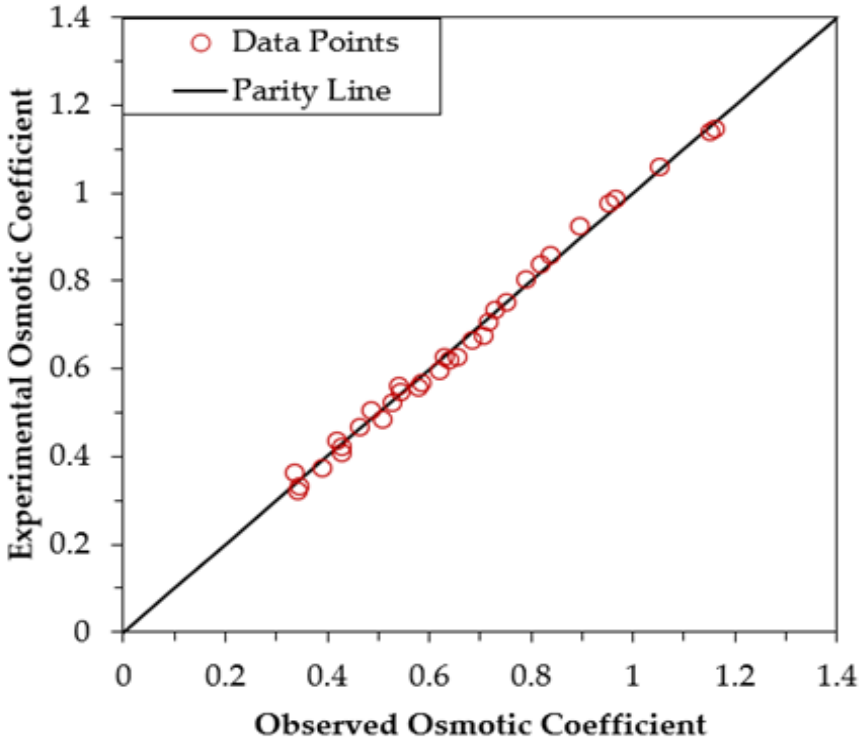

Fig 4.18. Parity plot of $MgSO_4$ for N=3

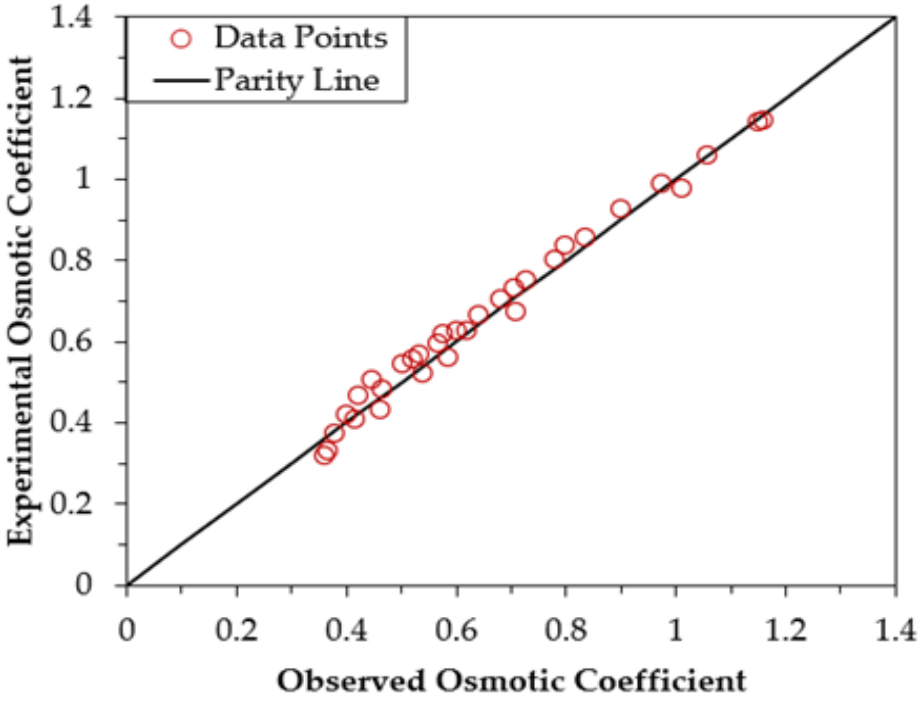

Fig 4.19. Parity plot of $MgSO_4$ for N=4

B. PHASE DIAGRAM GRAPH

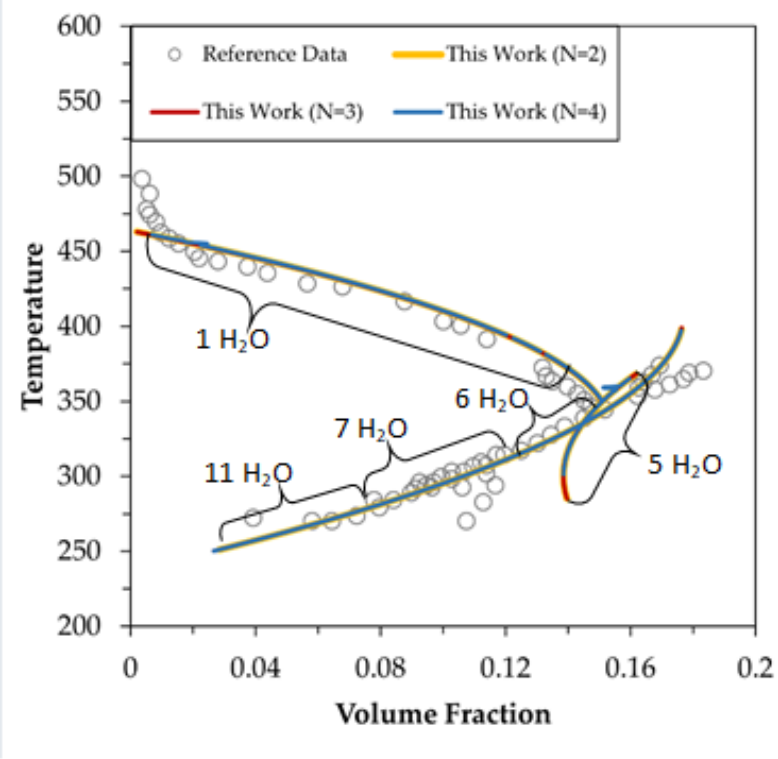

Fig 4.20. Phase diagram of the $MgSO_4$ + H_2O system
Symbols: experimental data reported in reference data [60,61,65,66,67]. Lines: the present model results

Fig 4.20. represents the phase diagram of $MgSO_4$ + H_2O system. The phase diagram for the $MgSO_4$ + H_2O system is more complex because there are more than three phases that can exist. In addition to the solid, liquid, and gas phases, there are also several hydrate phases. Those different hydrate include a count of 1, 4, 5, 6, 7 and 11 molecules of H_2O. The phase diagram for the $MgSO_4$ + H_2O system is useful for understanding the behaviour of this system in different conditions. For example, the diagram can be used to determine the conditions at which magnesium sulphate heptahydrate will form or decompose. This information can be used in a variety of applications, such as the production of magnesium sulphate and the desalination of water. Our model gave an excellent result of aligning with the experimental values for N=2, N=3 and N=4. There is a slight deviation from the experimental values in between the volume fraction of 0.0036 till 0.011.

Table-4.4 The comparison table for the critical point values from our work with reference values

	Our Work Data		**Reference Data**			
Salts	Critical Molality	Critical Temperature	Critical Molality	Critical Temperature	Temperature Deviation	References
$CaCl_2$	3.936351	229.065	4.4195	222.978	2.729865727	[55-59]
Li_2SO_4	3.450383	250.217	3.519	250.15	0.02678393	[52-54]
LiCl	8.682483	192.166	8.217	198.071	2.981254197	[52-54]
$MgSO_4$	1.841605	270.406	1.75	269.45	0.354796808	[60,65-67]
NaCl	4.958393	251.974	5.19	251.9	0.029376737	[52-53]

The above table provides us the data comparison of the critical points that we derived from our work vs the reference value. The critical point is the end point of a phase equilibrium curve in a phase diagram, and it marks the point where a substance's liquid and solid phases become indistinguishable. The critical point is important because it represents the conditions at which a substance undergoes a phase transition between the solid and liquid phases. With our model we got a small amount of deviation as mentioned in the table.

CHAPTER 5

SUMMARY AND CONCLUSION

The utilization of salt hydrates in thermochemical heat storage systems presents a promising avenue for achieving efficient and sustainable thermal energy storage, crucial for advancing renewable energy integration and addressing seasonal variations in energy generation. The exploration conducted in this paper underscores the significant potential of salt hydrates, such as sodium chloride, calcium chloride, and magnesium sulfate, lithium chloride, in efficiently storing and retrieving thermal energy.

Sensible heat storage, latent heat storage using phase change materials (PCMs), and thermochemical heat storage have all been investigated, with thermochemical heat storage standing out due to its high energy storage density and minimal heat loss during storage.

Furthermore, various models, including mean field theory and correlations derived from the Flory-Huggins theory and Extended Debye Huckel theory, have been employed to predict their thermodynamic properties, emphasizing the importance of precise experimental data for accurate modeling. Analysis of results revealed slight deviations between predictions and experimental data, with notable trends observed. Validation against experimental data confirmed the accuracy of our models, emphasizing their potential utility in predicting salt hydrate behavior accurately.

In summary, salt hydrates offer significant potential for efficient and sustainable thermal energy storage, promising to address challenges in renewable energy integration and contribute to a greener, more resilient energy infrastructure. By leveraging insights from experimental studies, thermodynamic modeling ,we can unlock the full potential of salt hydrates and pave the way towards a more sustainable future.

REFERENCES

1. Tatsidjodoung, P.; Le Pierrès, N.; Luo, L. Renewable and Sustainable Energy Reviews 2013, 18, 327.
2. Kalaiselvam S, Parameshwaran R. Seasonal thermal energy storage. Therm energystorageTechnolSustain-SystDesAssessAppl.ElsevierInc;2014.p.145–62.http://dx.doi.org/10.1016/B978-0-12-417291-3.00007-4.
3. GaoL,Zhao J, Tang Z. A review on bore hole seasonal solar thermal energy storage. Energyprocedia,vol.70.ElsevierB.V;2015.p.209–18. http://dx.doi. org/10.1016/j.egypro.2015.02.117.
4. Pinel P, Cruickshank Ca, Beausoleil-MorrisonI, Wills A. A review of available methods for seasonal storage of solar thermal energy in residential applications. Renew Sustain Energy Rev 2011;15:3341–59. http://dx.doi. org/10.1016/j.rser.2011.04.013.
5. Pielichowska K, Pielichowski K. Phase change materials for thermal energy storage. Prog Mater Sci 2014;65:67–123. http://dx.doi.org/10.1016/j. pmatsci.2014.03.005.
6. Nkwetta DN, Haghighat F. Thermal energy storage with phase change material- a state-of-the art review. Sustain Cities Soc 2014;10:87–100. http://dx.doi.org/10.1016/j.scs.2013.05.007.
7. Sharif MKA, Al-abidi AA, Mat S, Sopian K, Ruslan M H. Review of the application of phase change material for heating and domestic hot water systems. Renew Sustain Energy Rev 2015;42:557–68. http://dx.doi.org/ 10.1016/j.rser.2014.09.034.
8. P. Tatsidjodoung, N.L. Pierrs, L. Luo, A review of potential materials for thermal energy storage in building applications, Renew. Sustain. Energy Rev., 18 (2013), pp. 327-349
9. D. Aydin, S.P. Casey, S. Riffat, The latest advancements on thermochemical heat storage systems, Renew. Sustain. Energy Rev., 41 (2015), pp. 356-367
10. Blarke M B, Lund H. The effectiveness of storage and relocation options in renewable energy systems. Renew Energy 2008;33:1499–507. http://dx.doi. org/10.1016/j.renene.2007.09.001.
11. M. Gaeini, H.A. Zondag, C.C.M. Rindt, Effect of kinetics on the thermal performance of a sorption heat storage reactor, Applied Thermal Engineering, 102, (2016), 520-531
12. H. Zondag, A. Kalbasenka, M. van Essen, L. Bleijendaal, R. Schuitema, W. van Helden, L. Krosse, First studies in reactor concepts for thermochemical storage, Proc. Eurosun (2008)

13. Pinel, P.; Cruickshank, C. A.; Beausoleil-Morrison, I.; Wills, A. Renewable and Sustainable Energy Reviews 2011, 15, 3341.

14. Trausel, F et al., "A review on the properties of salt hydrates for thermochemical storage", SHC 2013, International Conference on Solar Heating and Cooling for Buildings and Industry September 23-25, 2013, Freiburg, Germany, Energy Procedia; 2014

15. Ali, H., Sarkisian, E.: Thermodynamics of vapor–liquid equilibrium in mixed solvent electrolyte sys tems. Sci. Iran **5**, 67–81 (1998)

16. Haghtalab, A., Vera, J.: A nonrandom factor model for the excess Gibbs energy of electrolyte solu tions. AIChE J. **34**, 803–813 (1988)

17. Holmes, H.F., Baes Jr., C.F., Mesmer, R.E.: Isopiestic studies of aqueous solutions at elevated temperatures I. KCl, $CaCl_2$, and $MgCl_2$. J. Chem. Thermodyn. **10**, 983–996 (1978)

18. Clegg, S.L., Pitzer, K.S., Brimblecombe, P.: Thermodynamics of multicomponent, miscible, ionic solutions. Mixtures including unsymmetrical electrolytes. J. Phys. Chem. **96**, 9470–9479 (1992)

19. Clegg, S.L., Pitzer, K.S.: Thermodynamics of multicomponent, miscible, ionic solutions: generalized equations for symmetrical electrolytes. J. Phys. Chem. **96**, 3513–3520 (1992)

20. Ghalami-Choobar, B., Mossayyebzadeh-Shalkoohi, P.: Activity coeffcient measurements and ther modynamic modeling of ($CaCl_2$+ l-alanine + water) system based on potentiometric determination at T = (298.2, 303.2, and 308.2) K. J. Chem. Eng. Data **60**, 2879–2894 (2015)

21. Ghalami-Choobar, B., Sayyadi-Nodehi, F.: Thermodynamic study of the (NaCl + serine + water) mixtures using potentiometric measurements at T = (298.2 and 303.2) K. Fluid Phase Equilib. **380**, 48–57 (2014)

22. Ghalami-Choobar, B., Mirzaie, S.: Thermodynamic study of (KCl + proline + water) system based on potentiometric measurements at T = (298.2 and 303.2) K. J. Mol. Liq. **169**, 124–129 (2012)

23. K. Linnow, M. Niermann, D. Bonatz, K. Posern, M. Steiger, Experimental studies of the mechanism and kinetics of hydration reactions, Energy Procedia, 48 (2014), pp. 394-404, 10.1016/j.egypro.2014.02.046

24. Piperopoulos, E.; Calabrese, L.; Bruzzaniti, P.; Brancato, V.; Palomba, V.; Caprì, A.; Frazzica, A.; Cabeza, L.F.; Proverbio, E.; Milone, C. Morphological and Structural Evaluation of Hydration/Dehydration Stages of MgSO4 Filled Composite Silicone Foam for Thermal Energy Storage Applications. Appl. Sci. 2020, 10, 453. https://doi.org/10.3390/app10020453

25. M. Gaeini, S.A. Shaik, C.C.M. Rindt, Characterization of potassium carbonate salt hydrate for thermochemical energy storage in buildings, Energy and Buildings, 196, (2019), 178-193

26. A.A. Hawwash, Hamdy Hassan, Khalid El feky, Impact of reactor design on the thermal energy storage of thermochemical Materials, Applied Thermal Engineering, 168, (2020), 114776

27. Wei Li, Qiuwang Wang, Min Zeng, Heat transformation performance of salt hydrate-based thermochemical energy storage sorbent during hydration, Cleaner Chemical Engineering, 1, (2022), 100006

28. Fenil Desai, Sunku Prasad Jenne, P. Muthukumar, Muhammad Mustafizur Rahman, Thermochemical energy storage system for cooling and process heating applications: A review, Energy Conversion and Management, 229, (2021), 113617

29. Changsheng Hao, Guosheng Feng, Changjie Ma, Camila Barreneche, Xiaohui She, Performance analysis of a novel multi-module columnar packed bed reactor with salt hydrates for thermochemical heat storage, Journal of Energy Storage, 86 (Part A), (2024), 111170

30. Hayatina I, Auckaili A, Farid M. Review on Salt Hydrate Thermochemical Heat Transformer. Energies. 2023; 16(12):4668. https://doi.org/10.3390/en16124668

31. Weisan Hua, Hongfei Yan, Xuelai Zhang, Xidong Xu, Liyu Zhang, Yao Shi, Review of salt hydrates-based thermochemical adsorption thermal storage technologies. Journal of Energy Storage, 56 (C), 106158 (2022)

32. Zhendong Ye, Hongzhi Liu, Wantong Wang, Han-Wen Liu, Jing Lv, Fan Yang, Reaction/sorption kinetics of salt hydrates for thermal energy storage, Journal of Energy Storage, 56(B), 106122 (2022)

33. Hui Yan Yang, Chengcheng Wang, Lige Tong, Shaowu Yin, Li Wang, Yulong Ding, Salt Hydrate Adsorption Material-Based Thermochemical Energy Storage for Space Heating Application: A Review, Energies 2023, 16(6), 2875; https://doi.org/10.3390/en16062875

34. Kenisarin, M., & Mahkamov, K. (2016). Salt hydrates as latent heat storage materials: Thermophysical properties and costs. Solar Energy Materials and Solar Cells, 145, 255-286.

35. Guillen, G. R., Pan, Y., Li, M., & Hoek, E. M. (2011). Preparation and characterization of membranes formed by nonsolvent induced phase separation: a review. Industrial & Engineering Chemistry Research, 50(7), 3798-3817.

36. S. K. Sharma, C. K. Jotshi, Amrao Singh, Density of molten salt hydrates—experimental data and an empirical correlation, The Canadian Journal of Chemical Engineering 65 (1987) 171-174

37. A. Minevich, Y. Marcus, and L. Ben-Dor, Densities of Solid and Molten Salt Hydrates and Their Mixtures and Viscosities of the Molten Salts, J. Chem. Eng. Data 49 (2004) 1451–1455

38. Joseph A. Rard, The Isopiestic Method: 100 Years Later and Still in Use, Journal of Solution Chemistry 48 (2019) 271–282

39. IngeRörig-Dalgaard, Direct Measurements of the Deliquescence Relative Humidity in Salt Mixtures Including the Contribution from Metastable Phases, ACS Omega 6 (2021) 16297−16306

40. Elena N. Tsurko, Roland Neueder and Werner Kun, Activity of Water, Osmotic and Activity Coefficients of Sodium Glutamate and Sodium Aspartate in Aqueous Solutions at 310.15 K, Acta Chim. Slov. 56 (2009) 58–64

41. Magin RL, Mangum BW, Statler JA, Thornton DD. Transition Temperatures of the Hydrates of Na2SO4, Na2HPO4, and KF as Fixed Points in Biomedical Thermometry. J Res Natl Bur Stand (1977). 1981 Mar-Apr;86(2):181-192. doi: 10.6028/jres.086.007. PMID: 34566042; PMCID: PMC6756278.

42. Archer, D. G., & Rard, J. A., Isopiestic Investigation of the Osmotic and Activity Coefficients of Aqueous MgSO4 and the Solubility of $MgSO_4$. $7H_2O$ (cr) at 298.15 K: Thermodynamic Properties of the $MgSO_4$+ H_2O System to 440 K. Journal of Chemical & Engineering Data, 43(5), (1998) 791-806.

43. Pitzer, K. S., & Shi, Y., Thermodynamics of calcium chloride in highly concentrated aqueous solution and in hydrated crystals. Journal of solution chemistry, 22, (1993) 99-105.

44. Monnin, C., Dubois, M., Papaiconomou, N., & Simonin, J. P., Thermodynamics of the LiCl+ H_2O system. Journal of Chemical & Engineering Data, 47(6), (2002) 1331-1336.

45. Kenneth S. Pitzer, Thermodynamics of electrolytes. I. Theoretical basis and general equations, J. Phys. Chem. 77 (2) (1973), 268–277

46. Pitzer, K.S. (1991). Activity Coefficients in Electrolyte Solutions (2nd ed.). CRC Press. https://doi.org/10.1201/9781351069472

47. Maojie Chai, Min Yang, Rundong Qi, Zhangxin Chen, Jing Li, Vapor-liquid equilibrium (VLE) prediction for dimethyl ether (DME) and water system in DME injection process with Peng-Robinson equation of state and composition dependent binary interaction coefficient, Journal of Petroleum Science and Engineering, 211, 110172 (2022)

48. Irong Nie, Ziwei Zheng, Mingxia Lu, Shun Yao, Dong Guo. Phase Behavior of Ionic Liquid-Based Aqueous Two-Phase Systems. International Journal of Molecular Sciences, (2022) ,23 (20), (2019) 12706. https://doi.org/10.3390/ijms232012706

49. Lalaso V. Mohite, Vinay A. Juvekar, Jyoti Sahu. Quantification of Polymer–Surface Interaction Using Microcalorimetry. Industrial & Engineering Chemistry Research, 58 (18), 7495-7510. https://doi.org/10.1021/acs.iecr.8b04792

50. Edgar J. Acosta, Arti S. Bhakta. The HLD-NAC Model for Mixtures of Ionic and Nonionic Surfactants. Journal of Surfactants and Detergents,12 (1), (2009) 7-19. https://doi.org/10.1007/s11743-008-1092-4

51. P.A.J. Donkers, L.C. Sögütoglu, H.P. Huinink, H.R. Fischer, O.C.G. Adan, A review of salt hydrates for seasonal heat storage in domestic applications, Applied Energy, **199**, 45-68(2017). https://doi.org/10.1016/j.apenergy.2017.04.080

52. Pielichowska, K.; Pielichowski, K. Phase change nanomaterials for thermal energy storage. In *Nanotechnology for Energy Sustainability*; Wiley: Hoboken, NJ, USA, pp. 459–484 (2017).

53. H. Lahmidi, S. Mauran, V. Goetz, Definition, test and simulation of a thermochemical storage process adapted to solar thermal systems, Sol. Energy 80 (7) (2006) 883–893

54. Li, D., Zeng, D., Yin, X., Han, H., Guo, L., & Yao, Y. Phase diagrams and thermochemical modeling of salt lake brine systems. II. NaCl+ H_2O, KCl+ H_2O, $MgCl_2$+ H_2O and $CaCl_2$+ H_2O systems. *Calphad*, *53*, (2016). 78-89.

55. Guendouzi, M. E., Mounir, A., & Dinane, A. (2003). Water activity, osmotic and activity coefficients of aqueous solutions of Li_2SO_4, Na_2SO_4, K_2SO_4,(NH_4) $2SO_4$, $MgSO_4$, $MnSO_4$, $NiSO_4$, $CuSO_4$, and $ZnSO_4$ at T= 298.15 K. *The Journal of Chemical Thermodynamics*, *35*(2), 209-220.

56. Pillay, V., Gärtner, R. S., Himawan, C., Seckler, M. M., Lewis, A. E., & Witkamp, G. J. (2005). $MgSO_4$+ H_2O System at Eutectic Conditions and Thermodynamic Solubility

Products of $MgSO_4$..$2H_2O$ (s) and $MgSO_4.7H_2O$ (s). *Journal of Chemical & Engineering Data*, *50*(2), 551-555.

57. Li, D., Zeng, D., Yin, X., & Gao, D. Phase diagrams and thermochemical modeling of salt lake brine systems. III. Li_2SO_4+ H_2O, Na_2SO_4+ H_2O, K_2SO_4+ H_2O, $MgSO_4$+ H_2O and $CaSO_4$+ H_2O systems. *Calphad*, *60*, (2018). 163-176.

58. Archer, D. G., & Rard, J. A. Isopiestic Investigation of the Osmotic and Activity Coefficients of Aqueous $MgSO_4$ and the Solubility of $MgSO_4.7H_2O$ (cr) at 298.15 K: Thermodynamic Properties of the $MgSO_4$+ H_2O System to 440 K. *Journal of Chemical & Engineering Data*, *43*(5), (1998). 791-806.

59. Yang, H., Zeng, D., Wang, Q., Chen, Y., & Voigt, W. Isopiestic measurements of water activity for the Li_2SO_4–$MgSO_4$–H_2O system at 323.15 and 373.15 K. *Journal of Chemical & Engineering Data*, *61*(9), 3157-3162, (2016).

60. Guendouzi, M. E., Mounir, A., & Dinane, A. Water activity, osmotic and activity coefficients of aqueous solutions of Li_2SO_4, Na_2SO_4, K_2SO_4,(NH_4) $2SO_4$, $MgSO_4$, $MnSO_4$, $NiSO_4$, $CuSO_4$, and $ZnSO_4$ at T= 298.15 K. *The Journal of Chemical Thermodynamics*, *35*(2), 209-220.(2003).

61. Monnin, C., Dubois, M., Papaiconomou, N., & Simonin, J. P. Thermodynamics of the LiCl+ H_2O system. *Journal of Chemical & Engineering Data*, *47*(6), (2002) 1331-1336.

62. Pátek, J., & Klomfar, J. Solid–liquid phase equilibrium in the systems of LiBr–H2O and LiCl–H2O. *Fluid Phase Equilibria*, *250*(1-2), (2006) 138-149.

63. Li, D., Zeng, D., Han, H., Guo, L., Yin, X., & Yao, Y. Phase diagrams and thermochemical modeling of salt lake brine systems. I. LiCl+ H_2O system. *Calphad*, *51*, 1-12(2015)..

64. Rard, J. A., Clegg, S. L., & Palmer, D. A.Isopiestic determination of the osmotic and activity coefficients of Li_2SO_4 (aq) at T= 298.15 and 323.15 K, and representation with an extended ion-interaction (Pitzer) model. *Journal of solution chemistry*, *36*,(2007). 1347-1371.

65. Hamer, W. J., & Wu, Y. C. Osmotic coefficients and mean activity coefficients of uni-univalent electrolytes in water at 25° C. *Journal of Physical and Chemical Reference Data*, *1*(4), 1047-1100(1972).

66. Rudakov, A. M., Sergievskii, V. V., & Nagovitsyna, O. A. Dependences of the osmotic coefficients of aqueous calcium chloride solutions on concentration at different temperatures. *Russian Journal of Physical Chemistry A*, *91*, 2361-2365 (2017).

67. Czerwienski, G. J. Osmotic and mean activity coefficients of $CaCl_2$, NaI, LiBr and LiCl in ethanol at 50 degrees C.

68. Partanen, J. I. (2012). Traceable mean activity coefficients and osmotic coefficients in aqueous calcium chloride solutions at 25 C up to a molality of 3.0 mol· kg–1. *Journal of Chemical & Engineering Data*, *57*(11), (1986) 3247-3257.

69. DUCKETT, L., HOLLIFIELD, J., & PATTERSON, C. Osmotic coefficients of aqueous CaCl2 solutions from 3 to 12 m at 50 oC. *Journal of chemical and engineering data*, *31*(2), (1986) 213-214.

70. Ananthaswamy, J., & Atkinson, G.Thermodynamics of concentrated electrolyte mixtures. 5. A review of the thermodynamic properties of aqueous calcium chloride in the temperature range 273.15-373.15 K. *Journal of Chemical and Engineering Data*, *30*(1), (1985) 120-128.

71. Gruszkiewicz, M. S., & Simonson, J. M. Vapor pressures and isopiestic molalities of concentrated CaCl2 (aq), CaBr2 (aq), and NaCl (aq) to T= 523 K. *The Journal of Chemical Thermodynamics*, *37*(9), (2005) 906-930.